AD-A116 729 NIELSEN ENGINEERING AND RESEARCH INC MOUNTAIN VIEW CA F/G 16/4
ANALYTICAL EXTENSION OF THE MISSILE1 AND MISSILE2 COMPUTER PROG--ETC(U)
MAR 82 M J HEMSCH, J MULLEN N00014-78-C-0388
UNCLASSIFIED NEAR-TR-272 NL

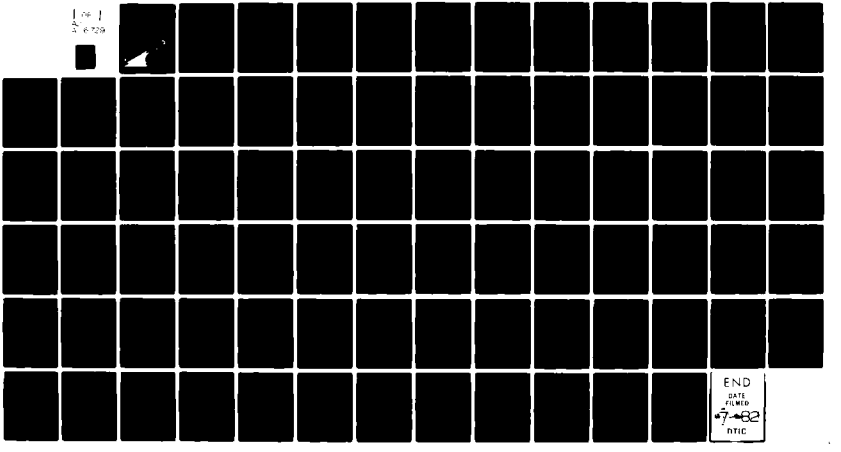

(12)

AD A116729

DTIC FILE COPY

NIELSEN ENGINEERING AND RESEARCH, INC.

OFFICES: 510 CLYDE AVENUE / MOUNTAIN VIEW, CALIFORNIA 94043 / TELEPHONE (415) 968-9457

COPY NO. 36

(12)

ANALYTICAL EXTENSION OF THE MISSILE1 AND MISSILE2 COMPUTER PROGRAMS

by

Michael J. Hemsch and Joseph Mullen, Jr.

NEAR TR 272
March 1982

Prepared under Contract No. N00014-78-C-0388

for

OFFICE OF NAVAL RESEARCH
Washington, DC

and

The Naval Weapons Center
China Lake, CA

by

NIELSEN ENGINEERING & RESEARCH, INC.
510 Clyde Avenue, Mountain View, CA 94043
Telephone (415) 968-9457

Unclassified

SECURITY CLASSIFICATION OF THIS PAGE (When Data Entered)

REPORT DOCUMENTATION PAGE		READ INSTRUCTIONS BEFORE COMPLETING FORM
1. REPORT NUMBER NEAR TR 272	2. GOVT ACCESSION NO.	3. RECIPIENT'S CATALOG NUMBER
4. TITLE (and Subtitle) ANALYTICAL EXTENSION OF THE MISSILE1 AND MISSILE2 COMPUTER PROGRAMS		5. TYPE OF REPORT & PERIOD COVERED Technical Report 7/1/81 to 12/31/81
		6. PERFORMING ORG. REPORT NUMBER
7. AUTHOR(s) MICHAEL J. HEMSCH JOSEPH MULLEN, JR.		8. CONTRACT OR GRANT NUMBER(s) N00014-78-C-0388 MOD. 4
9. PERFORMING ORGANIZATION NAME AND ADDRESS NIELSEN ENGINEERING & RESEARCH, INC. 510 Clyde Avenue Mountain View, CA 94043		10. PROGRAM ELEMENT, PROJECT, TASK AREA & WORK UNIT NUMBERS
11. CONTROLLING OFFICE NAME AND ADDRESS OFFICE OF NAVAL RESEARCH (Code 211) 800 N. Quincy Street Arlington, VA 22217		12. REPORT DATE March 1982
		13. NUMBER OF PAGES
14. MONITORING AGENCY NAME & ADDRESS(if different from Controlling Office)		15. SECURITY CLASS. (of this report) Unclassified
		15a. DECLASSIFICATION/DOWNGRADING SCHEDULE N/A

16. DISTRIBUTION STATEMENT (of this Report)

Approved for public release; distribution unlimited.

17. DISTRIBUTION STATEMENT (of the abstract entered in Block 20, if different from Report)

18. SUPPLEMENTARY NOTES

19. KEY WORDS (Continue on reverse side if necessary and identify by block number)

Missile aerodynamics
Guided missiles
Aerodynamic Characteristics

20. ABSTRACT (Continue on reverse side if necessary and identify by block number)

The range of application of the comprehensive set of missile aerodynamic prediction programs known as MISSILE1 and MISSILE2 has been analytically extended to M_∞=5 and fin AR=5. The extension is based on shock expansion theory applied to fins placed in body flow fields computed by an Euler equation solver. The results are normalized by wing-alone data obtained at NASA/LRC. Details of the method are presented in the report together with sample cases.

DD FORM 1 JAN 73 1473 EDITION OF 1 NOV 65 IS OBSOLETE

Unclassified

SECURITY CLASSIFICATION OF THIS PAGE (When Data Entered)

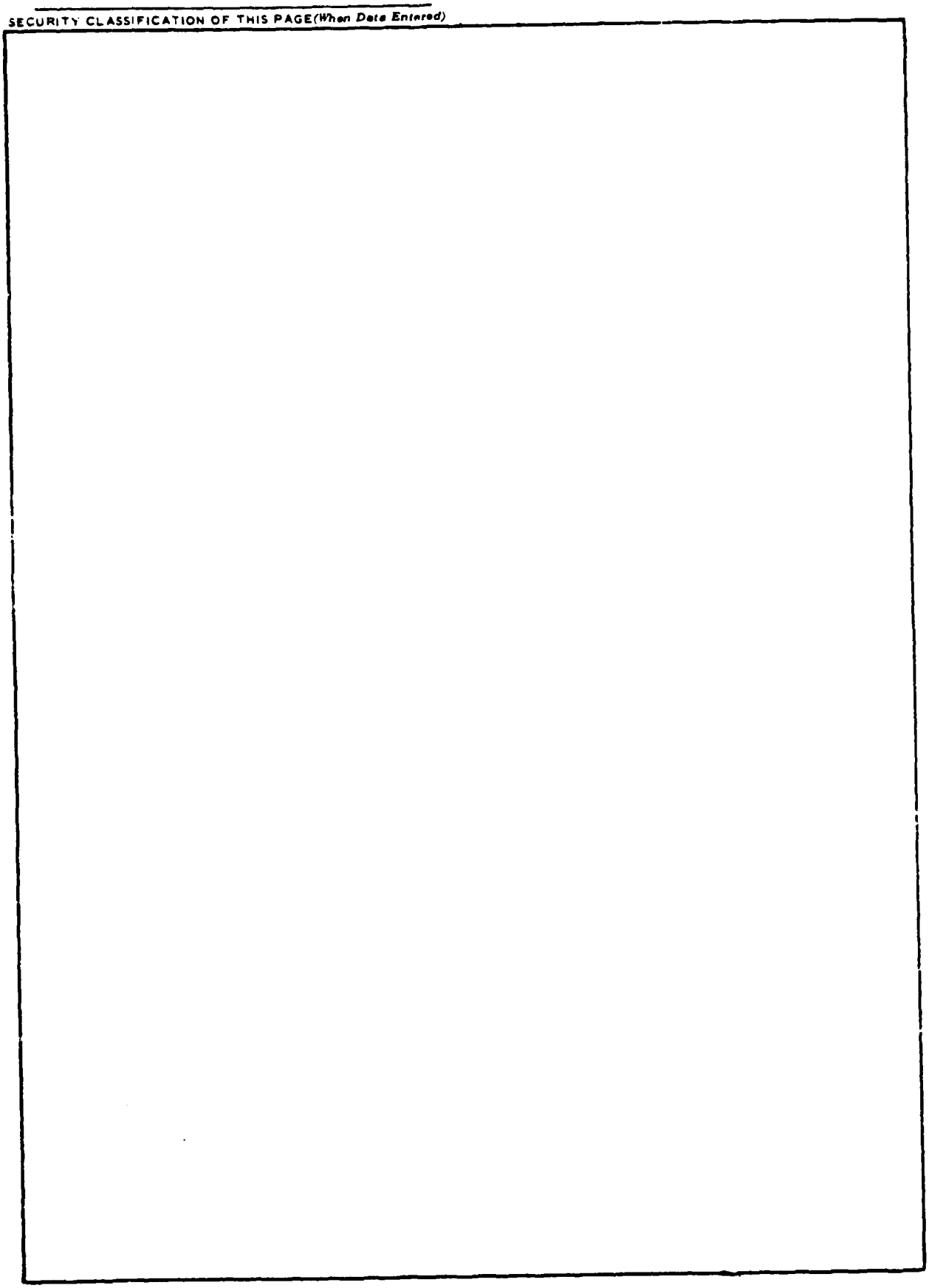

PREFACE

This technical report covers the work performed under Contract N00014-78-C-0388, Amendment P00004 from July 1, 1981 to December 31, 1981. Dr. Robert Whitehead is the Scientific Officer for the Office of Naval Research. Mr. R. E. Smith is the Technical Monitor for the Naval Weapons Center.

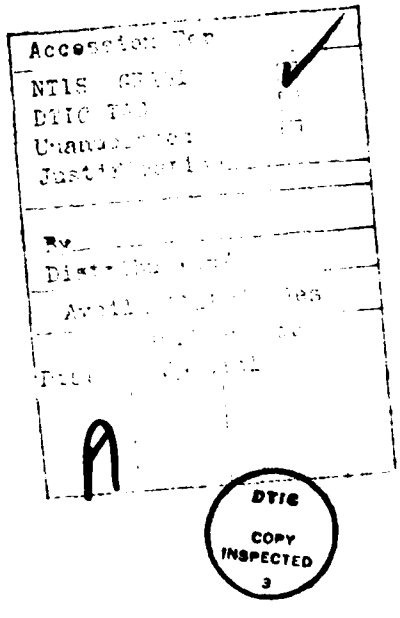

TABLE OF CONTENTS

1. INTRODUCTION

In 1977 and 1979, Nielsen Engineering & Research, Inc. (NEAR) released two new comprehensive missile aerodynamics prediction programs entitled MISSILE1 and MISSILE2 respectively (refs. 1 and 2). The codes are capable of computing the six component forces and moments acting on cruciform wing-body and wing-body-tail combinations with arbitrary roll and fin deflections. Individual fin (panel) loads are computed as well. The work was sponsored by the Office of Naval Research and the Naval Weapons Center.

The Mach number/fin aspect ratio domain covered by the two programs is shown in figure 1. The original boundaries of the domain are limited by the availability of systematic cruciform wing-body data for which panel loads were obtained since the codes use a semi-empirical approach requiring a fin-on-body data base. The domain is being extended in a program sponsored by all three services and NASA to be completed in 1984 (ref. 3). The purpose of the present work is to fulfill a Naval Weapons Center need for interim computer programs capable of handling Mach numbers up to five, fin aspect ratios up to 5, and angles of attack and fin deflection up to 20°. The work has been sponsored by NWC through the Office of Naval Research under contract N00014-78-C-0388.

The approach adopted for extending the fin data base was to use an existing Euler equation solver (ref. 4) to generate inviscid flow fields about a test body similar to the one used to obtain the present data base. Then, strip theory together with a wing-alone data base (ref. 5) was used to obtain loads on fins placed in the computed flow fields. Finally, the computed fin normal-force coefficients were adjusted to be consistent with the experimental data base already in the codes.

The rest of this report describes the details of the procedures used and gives some data comparisons made with the new codes designated MISSILE1A and MISSILE2A. Sample cases are also presented. Since the input requirements of the new codes have not been changed, the users manuals in references 1 and 2 are still applicable.

2. DEVELOPMENT OF ANALYTICAL EXTENSION

The steps involved in extending the fin data base are as follows:

1. Using an existing Euler equation solver, generate inviscid flow fields (i.e., without vortices) about a test body similar to the one used to generate the present experimental fin-on-body data base.
2. Compute the normal forces acting on fins placed in the flow fields of step 1 by using strip theory normalized by wing-alone data.
3. Adjust the computed normal-force coefficients to be consistent with the experimental data base already in the codes.

Step 1 involved running the Euler equation solver of reference 4 for angles of attack of 5°, 10°, 15°, and 20° and Mach numbers of 2.0, 3.0, and 4.5. Step 2 involved inserting the matrix of fins shown below into those twelve flow fields and computing the normal-force coefficients acting on them for roll angles varying from -90° to +90°. The T31, T14, T15, T11, and T23 fins are in the present data base generated by J. E. Fidler (ref. 6). They are in the matrix shown for two reasons: (1) the data base of reference 6 does not extend beyond M_∞ = 3.0 and (2) comparison of the computed and experimental coefficients at M_∞ = 2.0 and 3.0 gives necessary guidance for adjusting the computed results for the new conditions.

FIN MATRIX

AR \ λ	0	1/2	1
1/2		T31	
1	T14	T15	T11
2		T23	
4	T7	T8	T9

2.1 Fin-On-Body Normal Force Coefficients

2.1.1 Strip theory.- Simple strip theory gives the following result for the crossflow plane shown in the sketch below.

$$N_{strip} = \int_a^{s_m} c_n(\alpha_\ell, M_\ell) q_\ell c\,dt \qquad (1)$$

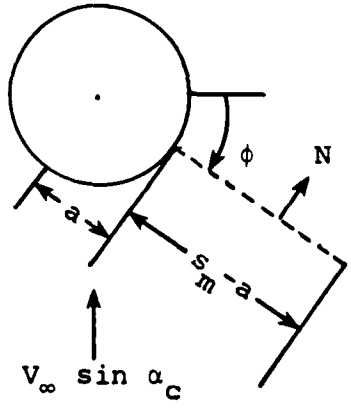

In equation (1) α_ℓ, M_ℓ, and q_ℓ are the local angle of attack, Mach number and dynamic pressure at the plane to be occupied by the fin as functions of spanwise distance from the body, t. The local angle of attack, α_ℓ, is defined in a plane normal to the fin chord plane.

Only zero-thickness fins are considered. The quantity c is the local fin chord and c_n is the local section normal-force coefficient given by 2-D shock-expansion theory. A subroutine written by F. K. Goodwin (ref. 7) was used to generate c_n.

To account for 3-D effects, we carry out the integration of (1) for some average α_ℓ and M_ℓ, divide (1) by that value and multiply by the experimental wing-alone value for $\bar{\alpha}_\ell$ and $\bar{M}_\ell$: i.e.,

$$N_{3\text{-}D} = C_{N_w}(\bar{\alpha}_\ell, \bar{M}_\ell)\bar{q}_\ell S \cdot \frac{N_{strip}}{N_{strip,\bar{\alpha}_\ell,\bar{M}_\ell}} \tag{2}$$

but

$$N_{strip,\bar{\alpha}_\ell,\bar{M}_\ell} = c_n(\bar{\alpha}_\ell, \bar{M}_\ell)\int_a^{s_m} q_\ell c\,dt \tag{3}$$

If we define $\bar{q}_\ell$ as

$$\bar{q}_\ell = \frac{1}{S}\int_a^{s_m} q_\ell c\,dt \tag{4}$$

and substitute (1), (3) and (4) into (2), we get

$$N_{3\text{-}D} = \frac{C_{N_w}(\bar{\alpha}_\ell, \bar{M}_\ell)}{c_n(\bar{\alpha}_\ell, \bar{M}_\ell)}\int_a^{s_m} c_n(\alpha_\ell, M_\ell) q_\ell c\,dt \tag{5}$$

Since the fin normal force coefficient is defined as

$$C_{N_{F(B)}} = \frac{N_{3\text{-}D}}{q_\infty S} \tag{6}$$

equation (5) can be rewritten as

$$C_{N_{F(B)}} = \frac{C_{N_w}(\bar{\alpha}_\ell, \bar{M}_\ell)}{c_n(\bar{\alpha}_\ell, \bar{M}_\ell)} \cdot \frac{1}{S} \cdot \int_a^{s_m} c_n(\alpha_\ell, M_\ell)\,\frac{q_\ell}{q_\infty}\,c\,dt \tag{7}$$

Equation (7) was used for all of the strip-theory calculations.

The development above does not suggest how to define $\bar{\alpha}_\ell$ and $\bar{M}_\ell$. Two obvious choices are (1) average over the span and (2) average over the span with c as a weighting parameter. Another possibility for $\bar{\alpha}_\ell$ is obtained by assuming c_n to be linear in α_ℓ and slowly varying with M_ℓ over the fin, i.e.,

$$c_n(\alpha_\ell, M_\ell) \approx c_{n_\alpha}(\bar{M}_\ell) \cdot \alpha_\ell \tag{8}$$

Substituting (8) into (1) gives

$$N_{strip} = c_{n_\alpha}(\bar{M}_\ell) \int_a^{s_m} \alpha_\ell q_\ell c\,dt \tag{9}$$

but substituting (8) into (3) gives

$$N_{strip,\bar{\alpha}_\ell,\bar{M}_\ell} = c_{n_\alpha}(\bar{M}_\ell)\bar{\alpha}_\ell \bar{q}_\ell S \tag{10}$$

Equating (9) and (10) gives

$$\bar{\alpha}_\ell = \frac{1}{\bar{q}_\ell S} \int_a^{s_m} \alpha_\ell q_\ell c\,dt \tag{11}$$

All of the averaging techniques described above were tried with virtually identical results. Another rather extreme approach is to replace c_n in (1) with $C_{N_w}(\alpha_\ell, M_\ell)$. If this is done, equation (7) simply becomes

$$C_{N_{F(B)}} = \frac{1}{S} \int_a^{s_m} C_{N_w}(\alpha_\ell, M_\ell) \frac{q_\ell}{q_\infty} c\,dt \tag{12}$$

Equations (7) and (12) gave nearly identical results.

2.1.2 Modification of strip theory results.- Fin T23 ($\mathcal{R}$ = 2, $\lambda = \frac{1}{2}$) was chosen to illustrate the accuracy of the Euler/strip-theory method. Figure 2 gives comparisons between the data now in MISSILE and the Euler/strip theory for M_∞ = 3.0 and the angle of attack range 5° to 20°. Note that the comparisons are good for the windward quadrant ($0 < \phi \leq 90°$) but the agreement for the leeward quadrant ($-90° \leq \phi \leq 0$) is unsatisfactory. The agreement for α_c = 15° appears to be fortuitous. Results for the other fins of interest are similar. Hence, we are forced to develop a procedure for improving the strip-theory results.

The method chosen is based on comparisons of the theory with data where available and extrapolating to the conditions of interest. The quantity to be extrapolated is

$$\varepsilon = \frac{C_{N_{F(B)}}\Big|_{data}}{C_{N_{F(B)}}\Big|_{Euler/strip\ theory}} \tag{13}$$

which is a function of α_c, ϕ and M_∞ for each fin. The steps involved are:

1. Extrapolate ε for α_c = 5°,10°,15°,20° and ϕ = -60°,-30°,0,30°,60° for each fin in the present data base (T31, T14, T15, T11, T23) from M_∞ = 2 and 3 to M_∞ = 4.5. Trial studies using wing-alone data (ref. 5) indicated that better results would be obtained if extrapolation were carried out linearly with respect to $1/\beta$ rather than M_∞ so that approach was adopted. The projected values of ε for M_∞ = 4.5 were multiplied by $C_{N_{F(B)}}\Big|_{Euler/strip\ theory}$ to get projected values of $C_{N_{F(B)}}\Big|_{data}$. Those results were plotted and hand-fit so that results for intermediate values of ϕ would be obtained. The final results are given in table 1 which is similar to those in ref. 1. Note that, as in ref. 1, results are given for α_c = 4° rather than α_c = 5°.

2. As in step 1, extrapolate ϵ for $\lambda = 1/2$ fins from $AR = 1$ and 2 to $AR = 4$ to obtain results for fin T8 ($AR = 4$, $\lambda = 1/2$) for $M_\infty = 2$ and 3. Trial studies using wing-alone data (ref. 5) indicated that better results would be obtained if extrapolation were carried out linearly in $\frac{1}{AR}$ rather than AR so that approach was adopted. The final results are given in tables 2 and 3.

3. As in step 1, extrapolate ϵ for fin T8 from $M_\infty = 2$ and 3 to $M_\infty = 4.5$. The final results are given in table 4.

Extrapolation for the $\lambda = 0$ and 1 fins (T7 and T9) from $AR = 1/2$ and 1 (see matrix on page 3) to $AR = 4$ was judged to be too risky. To account for taper ratio effects for the $AR = 4$ fins, the wing-alone data of ref. 5 were used in the following way:

1. The differences between the wing-along normal-force coefficients of the $AR = 2$ wings for $\lambda = 0$ and $\lambda = 1$ for $M_\infty = 2.0$, 3.0, and 4.5 were subtracted from the $\lambda = 1/2$ data for the same angle of attack.*

2. The differences found in step 1 were plotted versus C_{N_w} for the $\lambda = 1/2$ wing.

3. For a given α_c, ϕ, M_∞ combination the fin-on-body normal-force coefficient for the $AR = 4$, $\lambda = 1/2$ fins is found from tables 2(b), 3(b), and 4(b).

4. The result of step 3 is used in the results of step 2 to find the differences in fin-on-body normal-force coefficient due to taper ratios $\lambda = 0$ and 1.

The results of the above processes are given in tables 2-4.

2.1.3 Fin-body interference.- An important aspect of the MISSILE methodology is the equivalent angle-of-attack concept (ref. 1). That concept relies not only on a fin-on-body data base but also a data base for wings alone. To create the necessary additions to the wing-alone data base of ref. 1, we interpolated

*The wing-alone data of ref. 5 do not include taper ratio effects for the $AR = 4$ case.

and extrapolated in the data base of ref. 5. The results are given in table 5.

The factor in the α_{eq} concept which is used to account for the effects of fin span is K_W and is defined to be (ref. 1):

$$K_W = \frac{\tan \alpha_{eq}}{\tan \alpha_c} \tag{14}$$

where α_{eq} is given by

$$C_{N_W}(\alpha_{eq}) = C_{N_{F(B)}}(\alpha_c, \phi = 0, \delta = 0) \tag{15}$$

i.e., α_{eq} is the wing-alone angle of attack corresponding to $C_{N_{F(B)}}$ for zero roll and no fin deflections. Values of K_W for the data base extension are given in table 6.

2.2 Center-of-Pressure Location

Since no systematic fin-on-body force and moment data are available for $M_\infty > 3.0$ and since the Euler/strip theory was felt to be unreliable for center-of-pressure calculations, we resorted to using the wing-alone data of ref. 5 for $M_\infty \geq 2.0$. For both η and $\bar{x}/c_r$ the procedure used was as follows:

1. For each fin and M_∞ in the base of ref. 5, η and $\bar{x}$ were plotted versus C_{N_w}.
2. The curves from step 1 were crossplotted versus M_∞ with C_{N_w} as a parameter.
3. Values of η and $\bar{x}/c_r$ were obtained from the results of step 2 for M_∞ = 2.0, 3.0, and 4.5 for all fins in the data base.

The final results are given in tables 7 and 8.

2.3 Body-Vortex Data Base

The data base of reference 1 does not include forebody vortex information for $M_\infty > 3$. Hence, a study was conducted using the

Euler code of reference 4 with Kutta condition imposed to obtain vortex strengths for $M_\infty = 4.5$ and $\alpha_c = 10°,15°,20°$. Separation was started at x/D = 1.5 and at the meridional line given by $\phi = -30°$ for the entire length of the body in accordance with the correlation of ref. 8. The results are shown in figure 3 together with the previous correlation of ref. 1. Also shown are the experimental data of Oberkampf (ref. 9).

The comparisons of figure 3 convinced us to use the $M_\infty = 3$ correlation of reference 1 for all $M_\infty > 3$ as well.

3.0 DATA COMPARISONS AND SAMPLE CASES

The new additions to the data bases of references 1 and 2 as described above have been incorporated into the computer programs. The new codes have been designated MISSILE1A and MISSILE2A respectively. As a check on the accuracy of the new codes, results from MISSILE2A have been obtained for comparison with the AIM-9L wind tunnel data. The AIM-9L model is shown in figures 4 and 5. The test case was for $M_\infty = 3.5$, $\phi = 0$, $\delta_{1,3} = 20°$ (yaw) and $\delta_{2,4} = 0°$ (pitch). The comparisons are given in figure 6. Except for the rolling-moment coefficient the agreement is good. Note that for $M_\infty = 3.5$, the canard fin is well outside the data base of reference 1.

The sample cases for both codes were derived from the model of figures 4 and 5. The nose was approximated by a cone for convenience and $C_{N_\alpha}\Big|_{nose}$ was estimated to be 3.35 from available data. The sample cases represent the $\alpha_c = 20°$ data shown in figure 6. The sample inputs and outputs for MISSILE1A and 2A are given in figures 7 and 8 respectively. Since the input for both codes is unchanged, the users manuals for references 1 and 2 should still be used.

4.0 CONCLUSIONS

The data bases for the comprehensive missile aerodynamics prediction codes known as MISSILE1 and 2 have been extended by an analytical procedure using body-alone Euler finite-difference solutions, shock-expansion strip theory, wing-alone data and careful extrapolation. The fin data bases have been extended to $M_\infty = 4.5$ and $AR = 4$ for angles of attack up to 20°. The new codes designated MISSILE1A and 2A will allow cases for M_∞ up to five and AR up to five.

REFERENCES

1. Nielsen, J. N., Hemsch, M. J., and Smith, C. A.: A Preliminary Method For Calculating the Aerodynamic Characteristics of Cruciform Missiles to High Angles of Attack Including Effects of Roll Angle and Control Deflections. NEAR TR 152, ONR-CR215-226-4F, Nov. 1977. (MISSILE1)

2. Smith, C. A. and Nielsen, J. N.: Prediction of Aerodynamic Characteristics of Cruciform Missiles to High Angles of Attack Utilizing a Distributed Vortex Wake. NEAR TR 208, Jan. 1980. (MISSILE2)

3. Hemsch, M. J. and Nielsen, J. N.: Triservice Program for Extending Missile Aerodynamic Data Base and Prediction Program Using Rational Modeling. NEAR TR 249, Sept. 1981.

4. Klopfer, G. H. and Nielsen, J. N.: Basic Studies of Body Vortices at High Angles of Attack and Supersonic Speeds. NEAR TR 226, Oct. 1980.

5. Stallings, R. L., Jr. and Lamb, M.: Wing-Alone Aerodynamic Characteristics for High Angles of Attack at Supersonic Speeds. NASA TP 1889, Jul. 1981.

6. Derrick, J. N., Spring, D. J., and Winn, G. C.: Aerodynamic Characteristics of a Series of Bodies With and Without Tails at Mach Numbers From 0.8 to 3.0 and Angles of Attack from 0 to 45 Degrees. MICOM TR RD-7T-3, Jul. 1976.

7. Nielsen, J. N. and Goodwin, F. K.: A Preliminary Method for Estimating Hinge Moments of All-Movable Controls. NEAR TR 268, Mar. 1982.

8. Nielsen, J. N., Kuhn, G. D., and Klopfer, G. H.: Euler Solutions of Supersonic Wing-Body Interference at High Incidence Including Vortex Effects. NEAR TR 263, Jan. 1982.

9. Oberkampf, W.: Supersonic Flow Measurements in the Body Vortex Wakes of an Ogive Nose Cylinder. AFATL-TR-78-127, Nov. 1978.

10. Piper, E. M. and Brown, A. E.: AIM-9L Wind Tunnel Test Report, NWC TR 4063-233, Oct. 1972.

LIST OF SYMBOLS

a	body radius
AR	aspect ratio
C_ℓ	rolling-moment coefficient
C_m	pitching-moment coefficient
C_N	normal-force coefficient
$C_{N_{C(B)}}$	normal-force coefficient of two opposing canard fins on body
C_{N_W}	normal-force coefficient of wing alone
C_n	yawing-moment coefficient
C_Y	side-force coefficient
$C_{N_{F(B)}}$	normal-force coefficient of fin-on-body
c	local chord parallel to root chord
D	body diameter
K_W	interference coefficient for fin in presence of body
c_n	local section normal-force coefficient
M	Mach number
N	fin normal force
q	dynamic pressure
S	fin planform area
s_m	total fin semispan
V	flow velocity of free stream
x	distance from nose of body
α_c	angle of incidence of body

α_{eq} equivalent angle of attack

β $\sqrt{|M_\infty^2 - 1|}$

Γ vortex strength

δ_i deflection of fin i

ε ratio of experimental fin normal-force coefficient to that for Euler-strip theory.

λ fin taper ratio

ϕ roll angle measured clockwise from the horizontal plane (right fin down as viewed from rear)

Subscripts

ℓ local quantity

S separation

∞ free-stream condition

Table 1.- Fin-on-body normal-force coefficients without vortices present for $M_\infty = 4.5$ for fins in data base of references 1 and 2.

(a) Fin T31: AR = 1/2, $\lambda = 1/2$

$C_{N_{F(B)}}$ – fin normal-force coefficient

ϕ \ α_c	0°	4°	10°	15°	20°
-90°	0	0	0	0	0
-80°	0	.008	.015	.023	.025
-70°	0	.015	.027	.047	.053
-60°	0	.022	.040	.073	.085
-50°	0	.028	.055	.102	.125
-40°	0	.034	.070	.130	.165
-30°	0	.040	.085	.160	.205
-20°	0	.044	.105	.190	.247
-10°	0	.048	.123	.213	.285
0°	0	.051	.137	.233	.323
10°	0	.052	.148	.247	.353
20°	0	.054	.155	.253	.377
30°	0	.053	.155	.250	.388
40°	0	.051	.147	.230	.380
50°	0	.045	.132	.203	.340
60°	0	.037	.111	.165	.275
70°	0	.030	.080	.117	.185
80°	0	.017	.043	.062	.092
90°	0	0	0	0	0

Table 1.- Continued

(b) Fin T14: AR = 1, λ = 0

$C_{N_{F(B)}}$ – fin normal-force coefficient

ϕ \ α_c	0°	4°	10°	15°	20°
-90°	0	0	0	0	0
-80°	0	.006	.007	.015	.022
-70°	0	.012	.019	.035	.050
-60°	0	.019	.034	.056	.080
-50°	0	.026	.050	.080	.115
-40°	0	.032	.068	.106	.152
-30°	0	.039	.087	.134	.190
-20°	0	.044	.107	.161	.230
-10°	0	.048	.123	.187	.270
0°	0	.052	.137	.210	.300
10°	0	.052	.145	.232	.325
20°	0	.052	.147	.244	.342
30°	0	.050	.145	.245	.350
40°	0	.045	.140	.230	.340
50°	0	.038	.126	.206	.310
60°	0	.030	.106	.175	.265
70°	0	.022	.075	.125	.185
80°	0	.011	.040	.067	.095
90°	0	0	0	0	0

Table 1 ...tinued.

(c) Fin Tl ... AR = 1, λ = 1/2

$C_{N_{F(B)}}$ – fin n... al-force coefficient

ϕ \ α_c	0°	4°	10°	15°	20°
-90°	0	0	0	0	0
-80°	0	.010	.025	.030	.028
-70°	0	.020	.050	.055	.063
-60°	0	.030	.075	.085	.103
-50°	0	.038	.097	.111	.150
-40°	0	.046	.117	.140	.200
-30°	0	.054	.134	.166	.250
-20°	0	.060	.148	.195	.300
-10°	0	.064	.158	.220	.340
0°	0	.066	.165	.248	.372
10°	0	.068	.170	.263	.395
20°	0	.066	.169	.274	.410
30°	0	.062	.163	.275	.413
40°	0	.056	.153	.260	.397
50°	0	.048	.137	.231	.365
60°	0	.037	.112	.192	.312
70°	0	.026	.077	.136	.230
80°	0	.014	.040	.071	.125
90°	0	0	0	0	0

Table 1.- Continued.

(d) Fin T11: AR = 1, λ = 1

$C_{N_{F(B)}}$ – fin normal-force coefficient

ϕ \ α_c	0°	4°	10°	15°	20°
-90°	0	0	0	0	0
-80°	0	.008	.022	.036	.048
-70°	0	.016	.047	.071	.100
-60°	0	.026	.073	.105	.153
-50°	0	.036	.100	.138	.209
-40°	0	.044	.123	.170	.260
-30°	0	.052	.142	.202	.310
-20°	0	.058	.157	.230	.355
-10°	0	.060	.167	.260	.393
0°	0	.062	.175	.285	.426
10°	0	.060	.176	.304	.445
20°	0	.056	.174	.305	.455
30°	0	.050	.165	.194	.448
40°	0	.043	.143	.270	.422
50°	0	.036	.120	.235	.375
60°	0	.028	.093	.188	.310
70°	0	.020	.062	.130	.210
80°	0	.012	.030	.063	.110
90°	0	0	0	0	0

Table 1.- Concluded.

(e) Fin T23: $\mathcal{AR} = 2$, $\lambda = 1/2$

$C_{N_{F(B)}}$ – fin normal-force coefficient

ϕ \ α_c	0°	4°	10°	15°	20°
-90°	0	0	0	0	0
-80°	0	.006	.023	.035	.036
-70°	0	.014	.045	.072	.080
-60°	0	.022	.066	.107	.130
-50°	0	.029	.085	.140	.184
-40°	0	.036	.105	.172	.235
-30°	0	.042	.120	.205	.285
-20°	0	.048	.137	.235	.335
-10°	0	.053	.150	.265	.380
0°	0	.056	.162	.290	.425
10°	0	.058	.170	.302	.462
20°	0	.059	.170	.300	.485
30°	0	.057	.165	.287	.485
40°	0	.051	.145	.260	.450
50°	0	.043	.122	.222	.395
60°	0	.034	.095	.172	.312
70°	0	.023	.065	.117	.208
80°	0	.012	.032	.057	.105
90°	0	0	0	0	0

Table 2.- Fin-on-body normal-force coefficient without vortices present for $M_\infty = 2.0$ for $\mathcal{A}R = 4$ fins.

(a) Fin T7: $\lambda = 0$

$C_{N_{F(B)}}$ – fin normal-force coefficient

ϕ \ α_c	0°	4°	10°	15°	20°
-90°	0	0	0	0	0
-80°	0	.014	.025	.034	.050
-70°	0	.032	.072	.095	.140
-60°	0	.053	.134	.175	.245
-50°	0	.075	.205	.272	.375
-40°	0	.097	.286	.382	.500
-30°	0	.118	.370	.500	.625
-20°	0	.138	.434	.602	.735
-10°	0	.156	.475	.675	.830
0°	0	.172	.490	.725	.905
10°	0	.178	.490	.750	.925
20°	0	.175	.470	.745	.920
30°	0	.164	.432	.715	.890
40°	0	.144	.378	.632	.832
50°	0	.122	.315	.535	.740
60°	0	.096	.245	.430	.610
70°	0	.067	.170	.300	.425
80°	0	.034	.090	.160	.220
90°	0	0	0	0	0

Table 2.- Continued.

(b) Fin T8: $\lambda = 1/2$

$C_{N_{F(B)}}$ – fin normal-force coefficient

ϕ \ α_c	0°	4°	10°	15°	20°
-90°	0	0	0	0	0
-80°	0	.016	.020	.030	.070
-70°	0	.034	.048	.068	.165
-60°	0	.056	.110	.133	.275
-50°	0	.082	.230	.264	.410
-40°	0	.110	.334	.420	.550
-30°	0	.137	.410	.550	.690
-20°	0	.162	.467	.660	.806
-10°	0	.184	.505	.740	.900
0°	0	.200	.528	.790	.970
10°	0	.205	.526	.820	1.010
20°	0	.200	.510	.820	1.013
30°	0	.189	.477	.786	.985
40°	0	.169	.420	.710	.925
50°	0	.144	.355	.603	.824
60°	0	.112	.280	.478	.670
70°	0	.078	.190	.330	.470
80°	0	.039	.100	.170	.223
90°	0	0	0	0	0

Table 2.- Concluded.

(c) Fin T9: $\lambda = 1$

$C_{N_{F(B)}}$ – fin normal-force coefficient

ϕ \ α_c	0°	4°	10°	15°	20°
-90°	0	0	0	0	0
-80°	0	.016	.048	.056	.072
-70°	0	.036	.110	.140	.180
-60°	0	.059	.190	.240	.310
-50°	0	.085	.275	.348	.442
-40°	0	.110	.352	.455	.570
-30°	0	.134	.424	.562	.699
-20°	0	.157	.475	.650	.800
-10°	0	.177	.515	.730	.890
0°	0	.194	.540	.796	.967
10°	0	.201	.545	.824	1.004
20°	0	.198	.526	.825	1.006
30°	0	.185	.490	.793	.982
40°	0	.163	.426	.710	.920
50°	0	.137	.360	.614	.822
60°	0	.108	.282	.491	.680
70°	0	.075	.196	.355	.470
80°	0	.038	.100	.190	.240
90°	0	0	0	0	0

Table 3.- Fin-on-body normal-force coefficients without vortices present for $M_\infty = 3.0$ for $AR = 4$ fins.

(a) Fin T7: $\lambda = 0$

$C_{N_{F(B)}}$ – fin normal-force coefficient

ϕ \ α_c	0°	4°	10°	15°	20°
-90°	0	0	0	0	0
-80°	0	.008	.035	.038	.082
-70°	0	.018	.065	.080	.160
-60°	0	.028	.095	.128	.235
-50°	0	.039	.125	.180	.302
-40°	0	.051	.155	.232	.365
-30°	0	.061	.185	.285	.422
-20°	0	.072	.210	.340	.470
-10°	0	.082	.230	.382	.512
0°	0	.090	.250	.415	.555
10°	0	.094	.255	.428	.575
20°	0	.092	.246	.426	.585
30°	0	.084	.226	.400	.575
40°	0	.074	.194	.340	.490
50°	0	.062	.160	.280	.405
60°	0	.048	.120	.215	.315
70°	0	.033	.084	.145	.215
80°	0	.017	.045	.074	.110
90°	0	0	0	0	0

Table 3.- Continued.

(b) Fin T8: $\lambda = 1/2$

$C_{N_{F(B)}}$ – fin normal-force coefficient

ϕ \ α_c	0°	4°	10°	15°	20°
-90°	0	0	0	0	0
-80°	0	.006	.030	.040	.100
-70°	0	.016	.065	.090	.190
-60°	0	.027	.102	.146	.280
-50°	0	.041	.140	.212	.357
-40°	0	.056	.178	.275	.422
-30°	0	.070	.212	.334	.480
-20°	0	.084	.242	.385	.537
-10°	0	.094	.270	.435	.582
0°	0	.102	.294	.475	.622
10°	0	.104	.297	.496	.650
20°	0	.102	.287	.494	.665
30°	0	.094	.263	.458	.650
40°	0	.080	.222	.390	.570
50°	0	.068	.180	.322	.470
60°	0	.053	.136	.246	.365
70°	0	.036	.090	.167	.250
80°	0	.018	.045	.085	.130
90°	0	0	0	0	0

Table 3.- Concluded.

(c) Fin T9: $\lambda = 1$

$C_{N_{F(B)}}$ – fin normal-force coefficient

ϕ \ α_c	0°	4°	10°	15°	20°
-90°	0	0	0	0	0
-80°	0	.009	.035	.045	.100
-70°	0	.020	.070	.092	.192
-60°	0	.032	.104	.145	.288
-50°	0	.045	.140	.210	.360
-40°	0	.058	.180	.275	.440
-30°	0	.071	.217	.349	.512
-20°	0	.082	.250	.410	.570
-10°	0	.093	.280	.465	.620
0°	0	.104	.305	.507	.668
10°	0	.108	.305	.520	.695
20°	0	.104	.290	.515	.708
30°	0	.096	.270	.488	.691
40°	0	.084	.228	.410	.590
50°	0	.070	.185	.335	.490
60°	0	.054	.139	.252	.383
70°	0	.036	.092	.170	.250
80°	0	.018	.045	.082	.120
90°	0	0	0	0	0

Table 4.- Fin-on-body normal-force coefficients without voitices present for M_∞ - 4.5 for AR = 4 fins.

(a) Fin T7: $\lambda = 0$

$C_{N_{F(B)}}$ - fin normal-force coefficient

ϕ \ α_c	0°	4°	10°	15°	20°
-90°	0	0	0	0	0
-80°	0	.007	.030	.040	.055
-70°	0	.013	.050	.072	.105
-60°	0	.019	.070	.105	.155
-50°	0	.024	.090	.135	.200
-40°	0	.030	.108	.164	.248
-30°	0	.036	.120	.190	.290
-20°	0	.041	.135	.220	.335
-10°	0	.045	.148	.242	.378
0°	0	.048	.155	.265	.420
10°	0	.050	.160	.274	.460
20°	0	.050	.158	.270	.486
30°	0	.049	.154	.254	.484
40°	0	.044	.135	.224	.420
50°	0	.038	.110	.190	.350
60°	0	.030	.080	.145	.266
70°	0	.021	.060	.105	.182
80°	0	.011	.030	.055	.090
90°	0	0	0	0	0

Table 4.- Continued.

(b) Fin T8: $\lambda = 1/2$

$C_{N_{F(B)}}$ – fin normal-force coefficient

ϕ \ α_c	0°	4°	10°	15°	20°
-90°	0	0	0	0	0
-80°	0	.008	.024	.037	.055
-70°	0	.014	.046	.071	.110
-60°	0	.020	.068	.105	.165
-50°	0	.026	.088	.140	.220
-40°	0	.032	.108	.175	.273
-30°	0	.038	.125	.210	.325
-20°	0	.044	.143	.245	.380
-10°	0	.048	.157	.280	.435
0°	0	.052	.170	.312	.487
10°	0	.054	.178	.324	.527
20°	0	.054	.178	.318	.552
30°	0	.053	.170	.295	.557
40°	0	.047	.143	.255	.520
50°	0	.040	.115	.210	.420
60°	0	.032	.087	.160	.312
70°	0	.020	.058	.110	.205
80°	0	.010	.030	.055	.100
90°	0	0	0	0	0

Table 4.- Concluded.

(c) Fin T9: $\lambda = 1$

$C_{N_{F(B)}}$ — fin normal-force coefficient

ϕ \ α_c	0°	4°	10°	15°	20°
-90°	0	0	0	0	0
-80°	0	.008	.023	.040	.058
-70°	0	.014	.045	.075	.112
-60°	0	.020	.068	.107	.165
-50°	0	.026	.088	.146	.216
-40°	0	.032	.106	.180	.270
-30°	0	.038	.128	.219	.328
-20°	0	.044	.142	.248	.388
-10°	0	.048	.158	.280	.450
0°	0	.052	.176	.315	.507
10°	0	.054	.178	.320	.564
20°	0	.054	.180	.315	.600
30°	0	.053	.176	.298	.596
40°	0	.047	.150	.255	.505
50°	0	.040	.120	.210	.415
60°	0	.032	.088	.165	.315
70°	0	.020	.062	.106	.210
80°	0	.010	.030	.054	.105
90°	0	0	0	0	0

Table 5.- Wing-alone normal-force coefficients for new domain of data base.

FIN	T13	T14	T15	T11	T23		T7			T8			T9	
AR	1/2	1	1	1	2	←	4	→	←	4	→	←	4	→
λ	1/2	0	1/2	1	1/2	←	0	→	←	1/2	→	←	1	→
M_∞	4.5	4.5	4.5	4.5	4.5	2.0	3.0	4.5	2.0	3.0	4.5	2.0	3.0	4.5
$\alpha_{c'}$ deg														
0	0	0	0	0	0	0	0	0	0	0	0	0	0	0
2	.021	.025	.025	.029	.033	.066	.045	.035	.077	.051	.037	.074	.052	.037
4	.042	.049	.050	.057	.065	.131	.091	.069	.153	.102	.074	.149	.104	.074
6	.066	.075	.076	.092	.100	.203	.139	.108	.233	.157	.116	.231	.161	.118
8	.094	.103	.105	.132	.137	.281	.190	.152	.315	.217	.164	.321	.223	.170
10	.123	.131	.134	.172	.173	.359	.241	.195	.398	.277	.212	.412	.284	.221
12	.159	.168	.174	.213	.221	.426	.298	.231	.470	.343	.261	.483	.358	.267
14	.195	.204	.214	.253	.269	.494	.355	.266	.542	.409	.310	.554	.432	.313
16	.234	.240	.256	.296	.317	.559	.413	.309	.612	.472	.362	.624	.504	.367
18	.274	.276	.300	.340	.365	.622	.474	.360	.682	.533	.419	.692	.574	.430
20	.314	.313	.344	.385	.413	.684	.534	.411	.752	.594	.476	.760	.644	.493
22	.362	.361	.392	.441	.466	.748	.577	.469	.823	.647	.539	.828	.688	.565
24	.410	.409	.441	.496	.519	.812	.620	.528	.894	.700	.602	.897	.732	.637
26	.460	.459	.493	.548	.564	.870	.668	.592	.960	.755	.660	.958	.779	.706
28	.512	.511	.549	.596	.601	.923	.720	.661	1.022	.812	.712	1.011	.829	.773
30	.564	.563	.606	.644	.638	.976	.773	.730	1.084	.869	.763	1.064	.878	.839

Table 5.- Concluded

FIN	T13	T14	T15	T11	T23		T7			T8			T9	
AR	1/2	1	1	1	2	←	4	→	←	4	→	←	4	→
λ	1/2	0	1/2	1	1/2	←	0	→	←	1/2	→	←	1	→
	4.5	4.5	4.5	4.5	4.5	2.0	3.0	4.5	2.0	3.0	4.5	2.0	3.0	4.5
$\alpha_{c'}$ deg														
32	.620	.619	.670	.700	.717	1.031	.820	.763	1.132	.925	.816	1.120	.928	.869
34	.676	.675	.734	.756	.796	1.086	.866	.797	1.180	.981	.868	1.176	.978	.899
36	.734	.733	.797	.814	.867	1.134	.916	.841	1.219	1.035	.924	1.218	1.030	.942
38	.794	.793	.861	.874	.931	1.174	.969	.897	1.249	1.087	.984	1.246	1.082	.999
40	.853	.853	.924	.933	.996	1.214	1.022	.953	1.280	1.140	1.044	1.274	1.135	1.055
42	.913	.913	.988	.997	1.059	1.251	1.076	1.009	1.319	1.188	1.100	1.312	1.177	1.106
44	.973	.973	1.052	1.061	1.123	1.289	1.129	1.064	1.358	1.236	1.155	1.350	1.219	1.157
46	1.033	1.033	1.110	1.118	1.179	1.335	1.179	1.114	1.401	1.278	1.202	1.393	1.258	1.199
48	1.093	1.093	1.162	1.166	1.227	1.389	1.225	1.159	1.447	1.315	1.238	1.441	1.293	1.231
50	1.153	1.153	1.215	1.214	1.275	1.444	1.270	1.203	1.494	1.352	1.274	1.490	1.328	1.263
52	1.202	1.205	1.258	1.258	1.314	1.469	1.316	1.247	1.524	1.399	1.318	1.521	1.378	1.308
54	1.250	1.257	1.301	1.302	1.354	1.495	1.361	1.292	1.555	1.446	1.362	1.553	1.428	1.352
56	1.296	1.303	1.343	1.344	1.390	1.523	1.400	1.338	1.583	1.487	1.408	1.581	1.469	1.402
58	1.340	1.343	1.383	1.384	1.422	1.555	1.431	1.388	1.609	1.521	1.455	1.604	1.501	1.457
60	1.383	1.383	1.422	1.423	1.454	1.586	1.464	1.437	1.635	1.555	1.503	1.627	1.533	1.512

Table 6.- Values of K_W for the data base extension.

(a) Fins in old data base; $M_\infty = 4.5$

FIN	T31	T14	T15	T11	T23
AR	1/2	1	1	1	2
λ	1/2	0	1/2	1	1/2
α_c					
4°	1.179	1.048	1.293	1.066	.855
10°	1.075	1.029	1.152	1.011	.931
15°	1.064	.953	1.039	1.031	.987
20°	1.010	.960	1.060	1.078	1.021

(b) Fin T7; AR = 4, $\lambda = 0$

M_∞	2.0	3.0	4.5
α_c			
4°	1.082	.988	.687
10°	1.372	1.025	.810
15°	1.417	1.068	.922
20°	1.385	1.046	1.014

Table 6.- Concluded.

(c) Fin T8; AR = 4, λ = 1/2

M_∞	2.0	3.0	4.5
α_c			
4°	1.262	.998	.700
10°	1.343	1.046	.819
15°	1.400	1.070	.933
20°	1.327	1.052	1.017

(d) Fin T9; AR = 4, λ = 1

M_∞	2.0	3.0	4.5
α_c			
4°	1.239	1.000	.694
10°	1.354	1.050	.819
15°	1.408	1.070	.933
20°	1.329	1.053	1.018

Table 7.- Values of $\bar{x}/c_r$ for wing-alone results of ref. 5.

(a) AR = 1/2, λ = 0

C_N \ M_∞	2.0	3.0	4.5
0	.675	.669	.644
0.2	.653	.646	.641
0.4	.648	.643	.640
0.6	.645	.642	.640
0.8	.644	.642	.640
1.0	.640	.643	.645
1.2	.639	.645	.648
1.4	.638	.645	.651
1.6	.638	.647	.660

(b) AR = 1, λ = 0

C_N \ M_∞	2.0	3.0	4.5
0	.666	.648	.631
0.2	.653	.636	.620
0.4	.645	.635	.626
0.6	.642	.635	.632
0.8	.641	.639	.636
1.0	.639	.640	.640
1.2	.633	.639	.640
1.4	.630	.636	.638
1.6	.627	.631	.632

Table 7.- Continued.

(c) AR = 2, λ = 0

C_N \ M_∞	2.0	3.0	4.5
0	.648	.620	.600
0.2	.637	.614	.604
0.4	.630	.615	.609
0.6	.628	.620	.618
0.8	.630	.627	.626
1.0	.627	.629	.629
1.2	.624	.630	.632
1.4	.622	.626	.628
1.6	.630	.630	.630

(d) AR = 1/2, λ = 1/2

C_N \ M_∞	2.0	3.0	4.5
0	.522	.545	.519
0.2	.533	.556	.547
0.4	.557	.564	.563
0.6	.561	.569	.569
0.8	.564	.571	.572
1.0	.566	.574	.574
1.2	.568	.576	.576
1.4	.569	.577	.577
1.6	.570	.579	.579

Table 7.- Continued.

(e) AR = 1, λ = 1/2

C_N \ M_∞	2.0	3.0	4.5
0	.523	.515	.459
0.2	.535	.527	.504
0.4	.544	.541	.530
0.6	.552	.553	.547
0.8	.558	.560	.558
1.0	.560	.563	.564
1.2	.562	.565	.566
1.4	.564	.567	.568
1.6	.564	.567	.568

(f) AR = 2, λ = 1/2

C_N \ M_∞	2.0	3.0	4.5
0	.480	.475	.459
0.2	.496	.489	.482
0.4	.511	.503	.495
0.6	.527	.518	.515
0.8	.536	.532	.531
1.0	.541	.544	.544
1.2	.541	.548	.548
1.4	.552	.554	.554
1.6	.577	.578	.578

Table 7.- Continued.

(g) AR = 4, λ = 1/2

C_N \ M_∞	2.0	3.0	4.5
0	.450	.443	.432
0.2	.463	.458	.450
0.4	.477	.473	.468
0.6	.492	.487	.485
0.8	.507	.504	.502
1.0	.515	.519	.521
1.2	.523	.536	.538
1.4	.544	.554	.556
1.6	.572	.574	.574

(h) AR = 1/2, λ = 1

C_N \ M_∞	2.0	3.0	4.5
0	.295	.346	.309
0.2	.345	.370	.354
0.4	.383	.388	.384
0.6	.404	.406	.407
0.8	.418	.422	.424
1.0	.428	.435	.438
1.2	.439	.446	.444
1.4	.446	.454	.455
1.6	.451	.462	.457

Table 7.- Concluded.

(i) $\mathcal{R} = 1$, $\lambda = 1$

C_N \ M_∞	2.0	3.0	4.5
0	.330	.344	.309
0.2	.352	.362	.341
0.4	.371	.378	.368
0.6	.388	.394	.389
0.8	.402	.408	.407
1.0	.415	.420	.421
1.2	.428	.432	.432
1.4	.436	.440	.439
1.6	.448	.448	.444

(j) $\mathcal{R} = 2$, $\lambda = 1$

C_N \ M_∞	2.0	3.0	4.5
0	.320	.316	.240
0.2	.336	.336	.306
0.4	.358	.353	.336
0.6	.373	.369	.358
0.8	.390	.385	.378
1.0	.406	.400	.397
1.2	.418	.417	.416
1.4	.433	.434	.434
1.6	.444	.455	.452

Table 8.- Values of η for wing-alone results of ref. 5.

(a) $AR = 1/2$, $\lambda = 0$

C_N \ M_∞	2.0	3.0	4.5
0	.396	.377	.361
0.2	.356	.338	.325
0.4	.336	.324	.321
0.6	.323	.320	.320
0.8	.317	.318	.320
1.0	.314	.317	.320
1.2	.312	.317	.320
1.4	.312	.317	.320
1.6	.312	.317	.320

(b) $AR = 1$, $\lambda = 0$

C_N \ M_∞	2.0	3.0	4.5
0	.414	.392	.380
0.2	.384	.353	.333
0.4	.352	.332	.325
0.6	.334	.325	.323
0.8	.327	.323	.321
1.0	.322	.320	.320
1.2	.315	.317	.319
1.4	.312	.315	.317
1.6	.312	.315	.317

Table 8.- Continued.

(c) $\mathcal{R} = 2$, $\lambda = 0$

C_N \ M_∞	2.0	3.0	4.5
0	.385	.379	.390
0.2	.373	.359	.365
0.4	.359	.342	.339
0.6	.344	.334	.331
0.8	.332	.328	.327
1.0	.323	.323	.323
1.2	.315	.319	.319
1.4	.311	.316	.316
1.6	.311	.315	.315

(d) $\mathcal{R} = 1/2$, $\lambda = 1/2$

C_N \ M_∞	2.0	3.0	4.5
0	.463	.440	.439
0.2	.475	.454	.432
0.4	.460	.436	.427
0.6	.440	.431	.426
0.8	.431	.429	.427
1.0	.427	.427	.427
1.2	.424	.426	.426
1.4	.422	.425	.426
1.6	.422	.425	.426

Table 8.- Continued.

(e) AR = 1, λ = 1/2

C_N \ M_∞	2.0	3.0	4.5
0	.409	.424	.453
0.2	.431	.438	.441
0.4	.447	.435	.432
0.6	.447	.433	.427
0.8	.441	.430	.427
1.0	.432	.428	.427
1.2	.426	.426	.427
1.4	.423	.425	.427
1.6	.422	.424	.427

(f) AR = 2, λ = 1/2

C_N \ M_∞	2.0	3.0	4.5
0	.428	.444	.441
0.2	.433	.454	.451
0.4	.433	.452	.454
0.6	.433	.438	.442
0.8	.433	.432	.433
1.0	.430	.429	.429
1.2	.428	.427	.427
1.4	.426	.427	.427
1.6	.425	.427	.427

Table 8.- Continued.

(g) AR = 4, λ = 1/2

C_N \ M_∞	2.0	3.0	4.5
0	.419	.436	.449
0.2	.442	.449	.450
0.4	.445	.452	.453
0.6	.437	.452	.454
0.8	.435	.440	.443
1.0	.432	.435	.436
1.2	.433	.434	.432
1.4	.433	.434	.431
1.6	.433	.433	.431

(h) AR = 1/2, λ = 1

C_N \ M_∞	2.0	3.0	4.5
0	.463	.458	.449
0.2	.482	.472	.466
0.4	.490	.479	.475
0.6	.491	.483	.482
0.8	.489	.485	.484
1.0	.487	.485	.485
1.2	.486	.485	.485
1.4	.486	.485	.485
1.6	.486	.485	.485

Table 8.- Concluded.

(i) AR = 1, λ = 1

C_N \ M_∞	2.0	3.0	4.5
0	.436	.447	.444
0.2	.454	.460	.459
0.4	.469	.470	.470
0.6	.478	.478	.478
0.8	.483	.482	.482
1.0	.485	.484	.484
1.2	.487	.485	.485
1.4	.488	.486	.486
1.6	.488	.486	.486

(j) AR = 2, λ = 1

C_N \ M_∞	2.0	3.0	4.5
0	.430	.450	.451
0.2	.447	.465	.467
0.4	.460	.469	.472
0.6	.469	.474	.476
0.8	.476	.478	.480
1.0	.481	.481	.482
1.2	.485	.485	.485
1.4	.488	.488	.487
1.6	.489	.488	.489

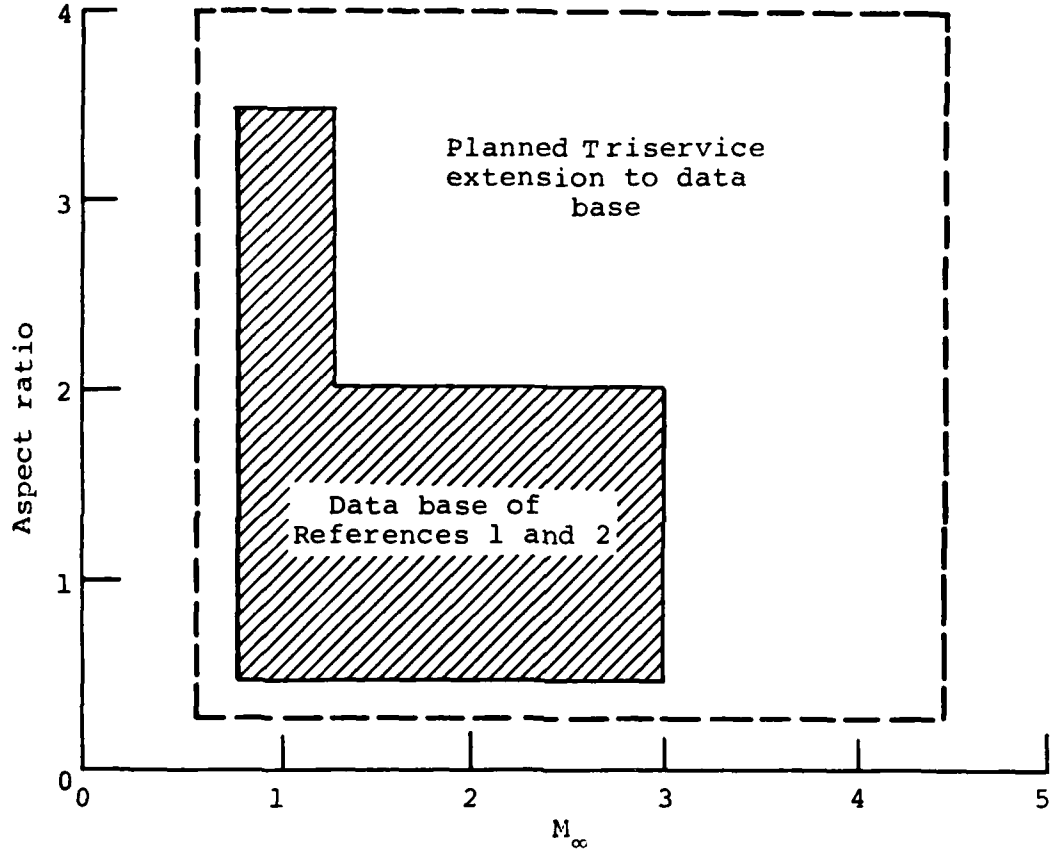

Figure 1.- Aspect ratio-Mach number range of MISSILE1 and MISSILE2 and planned Triservice extensions.

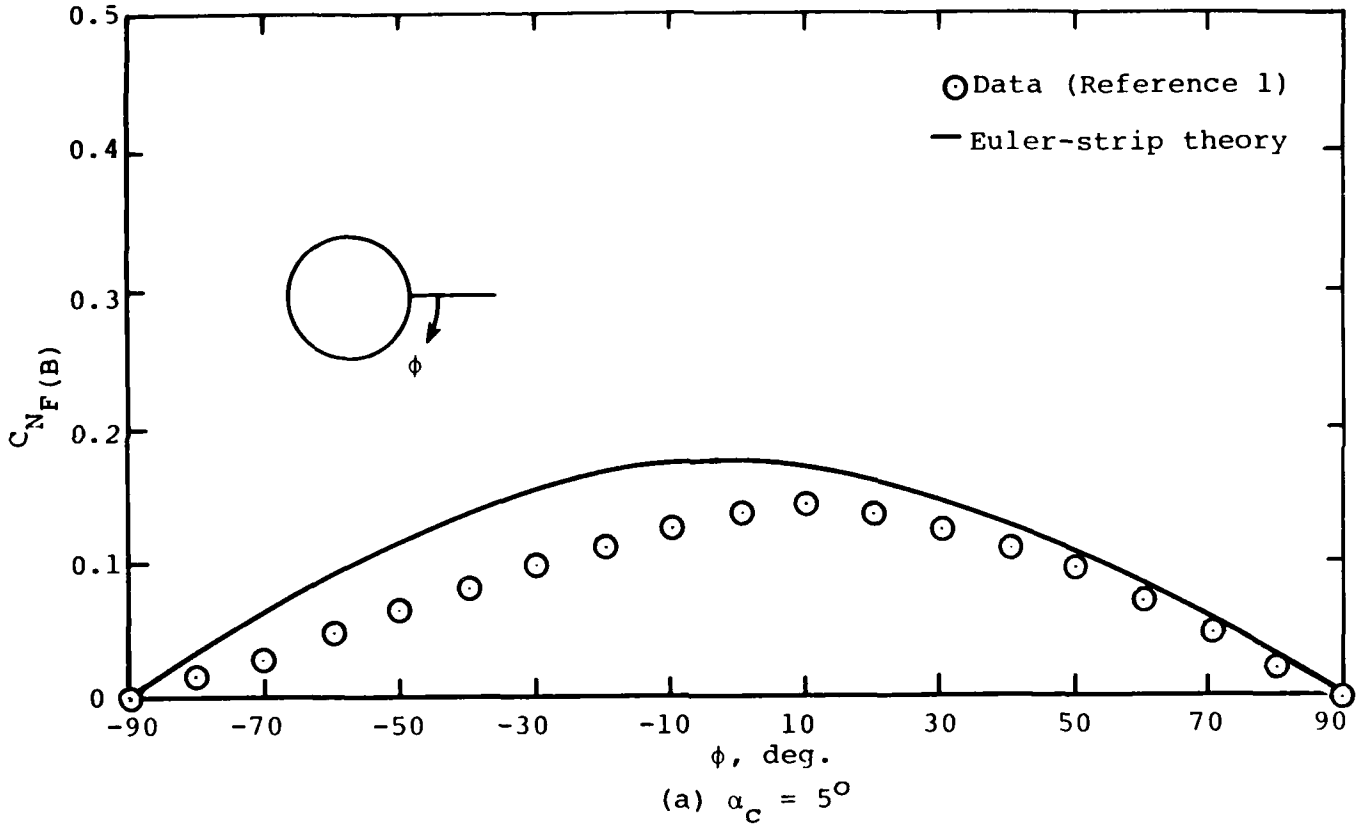

(a) $\alpha_c = 5^o$

Figure 2.- Comparison between experiment and Euler-strip theory for T23 fin; $M_\infty = 3.0$, AR = 2, $\lambda = \frac{1}{2}$.

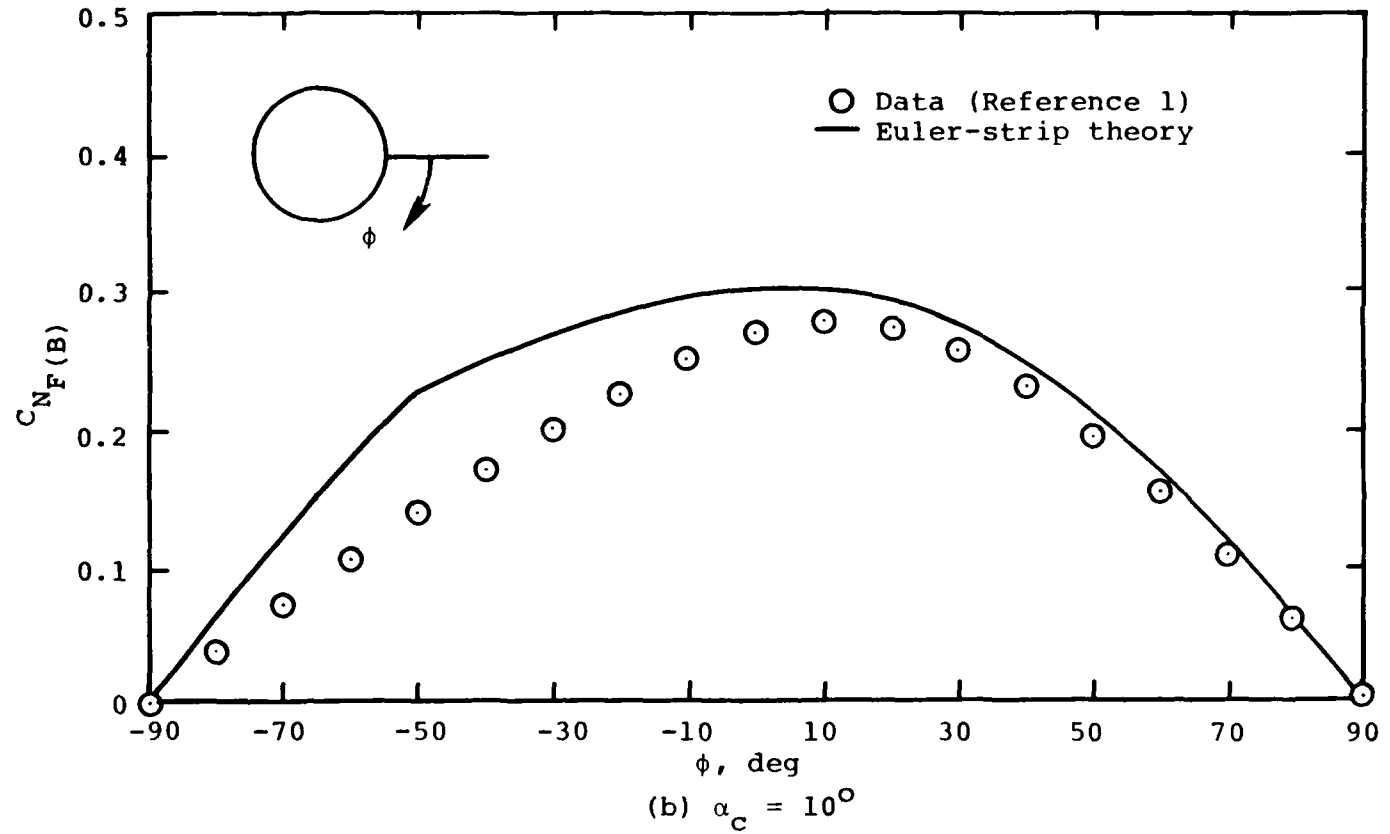

(b) $\alpha_c = 10^o$

Figure 2.- Continued.

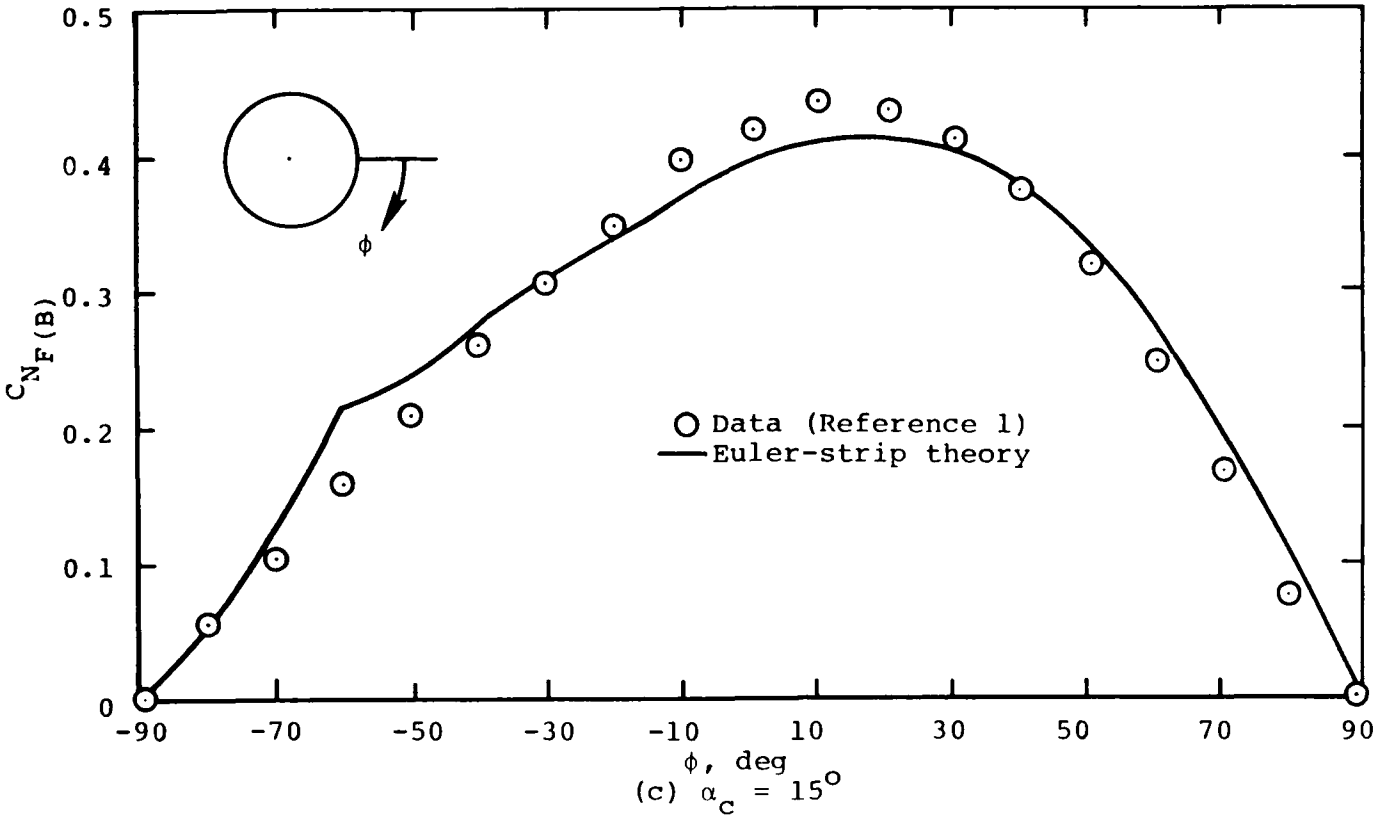

(c) $\alpha_c = 15^o$

Figure 2.- Continued.

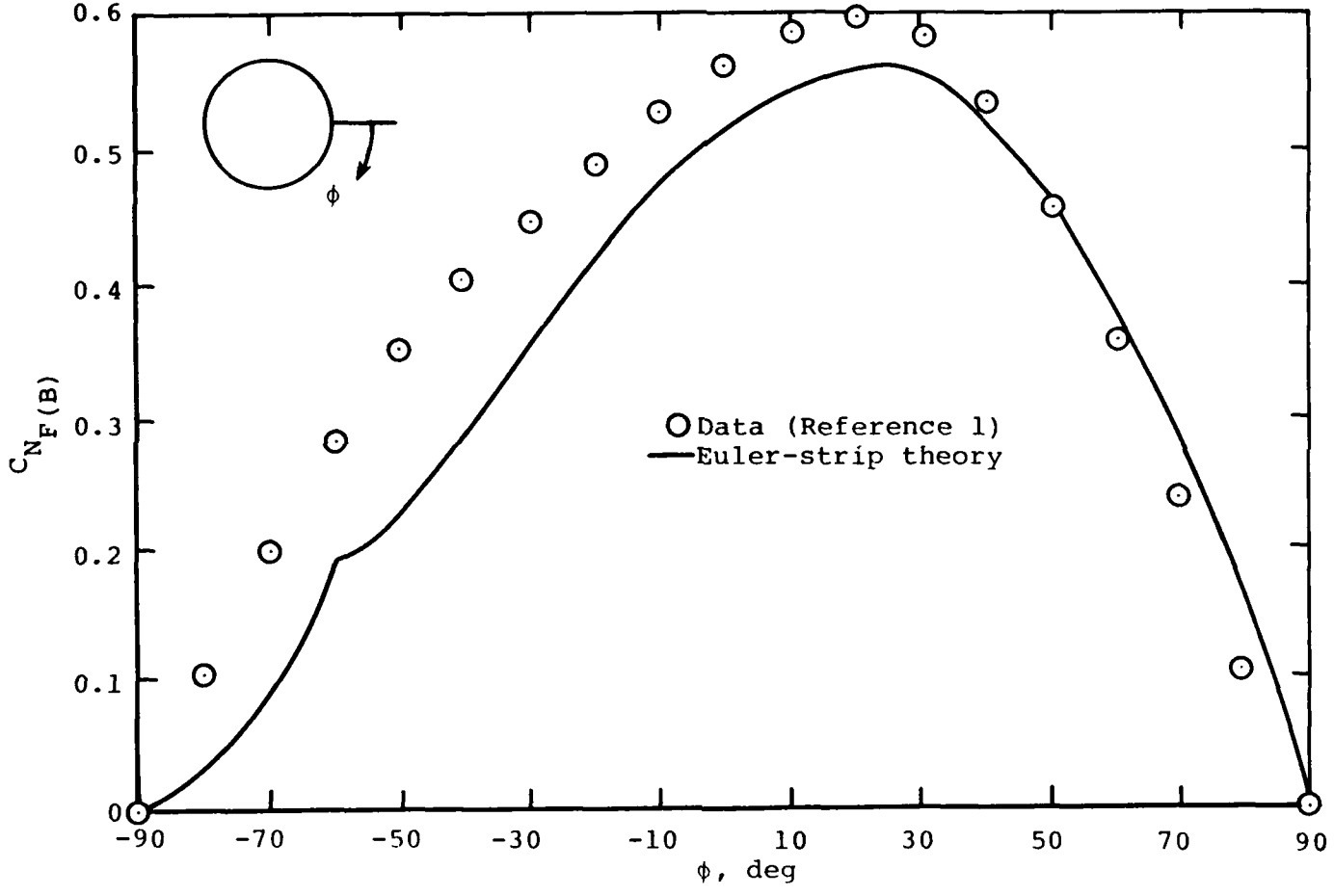

(d) $\alpha_c = 20^o$

Figure 2.- Concluded.

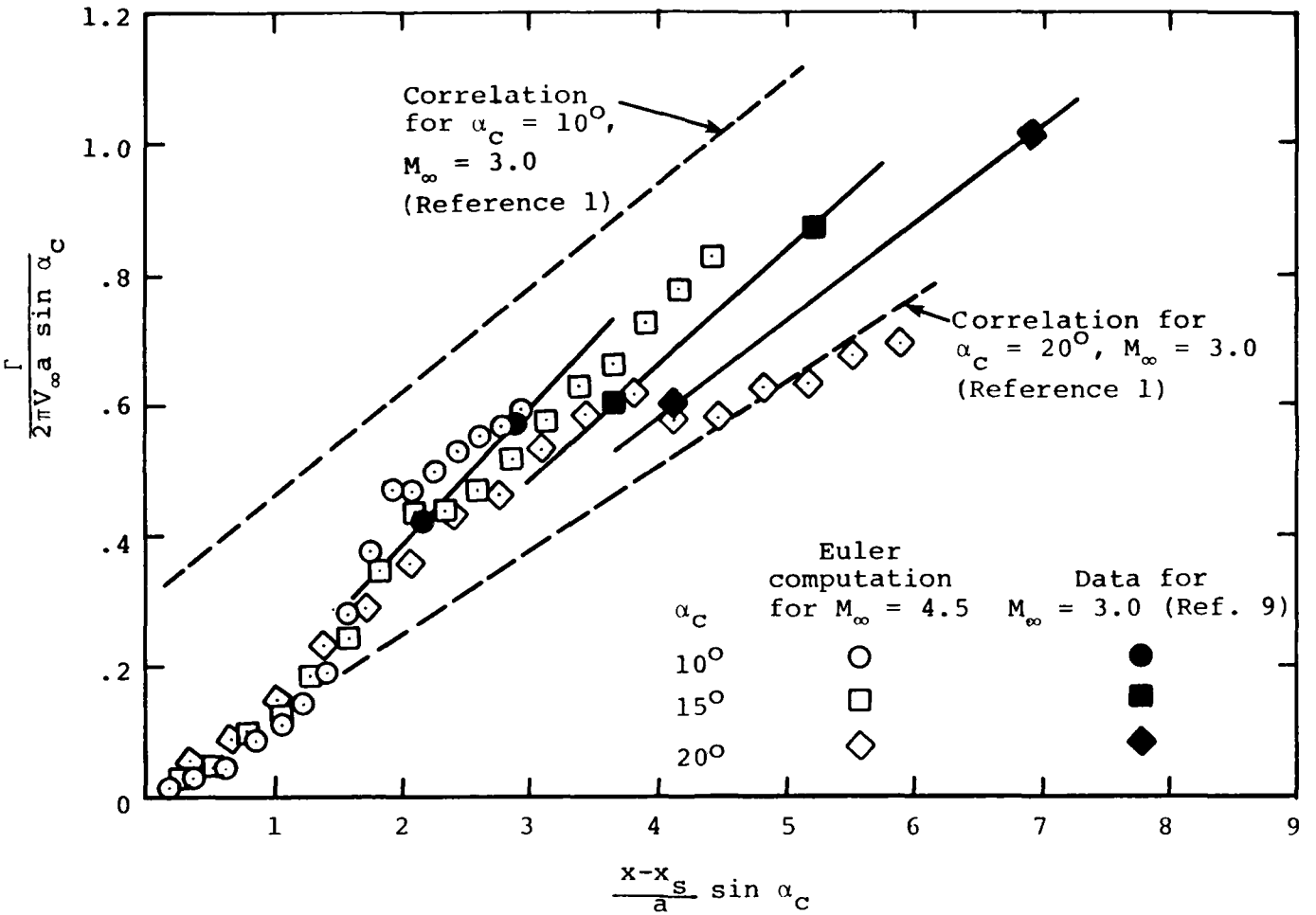

Figure 3.- Comparison of correlations from reference 1, data from reference 8 and Euler computation for forebody vortex strengths; $M_\infty = 4.5$ tangent-ogive cylinder with $L_N/D = 3$.

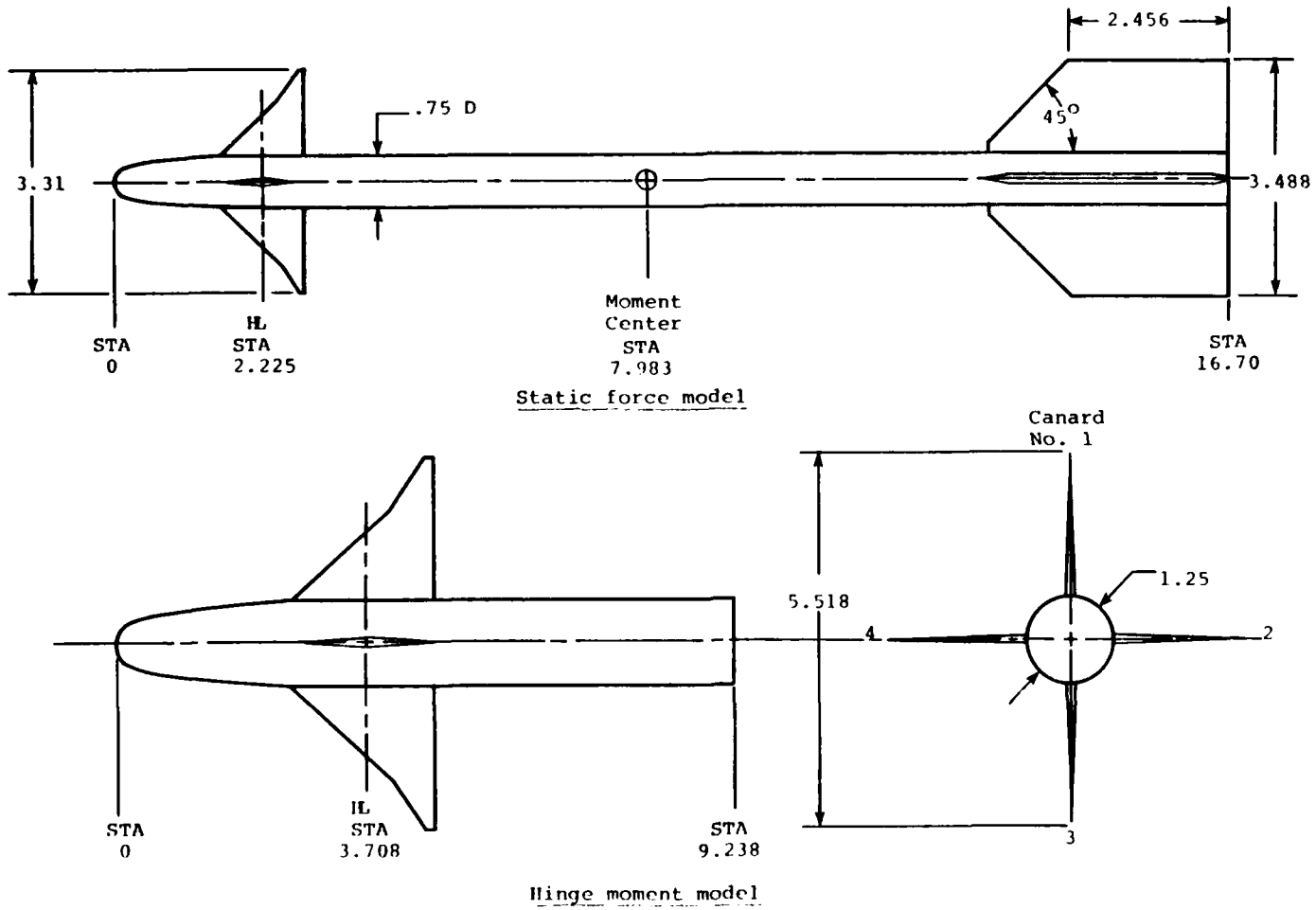

Figure 4.- AIM-9L wind tunnel models.

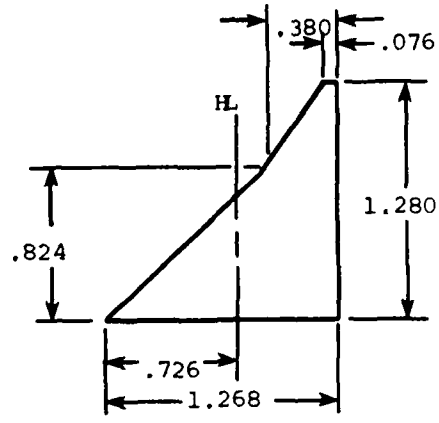

Static force model

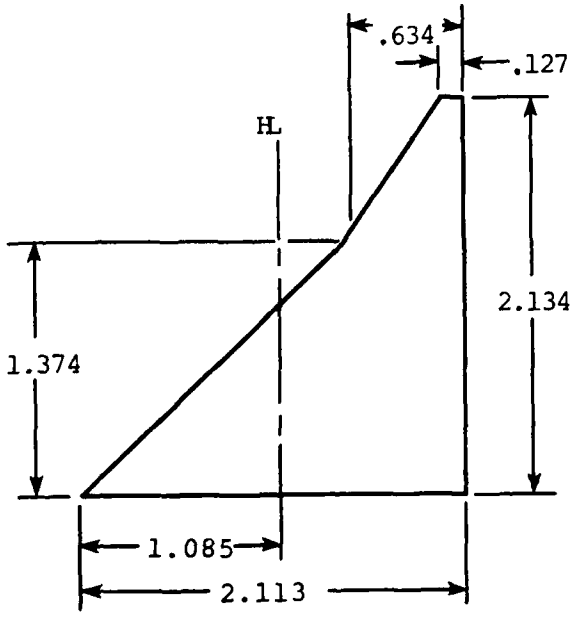

Hinge moment model

Figure 5.- Canard planform geometry.

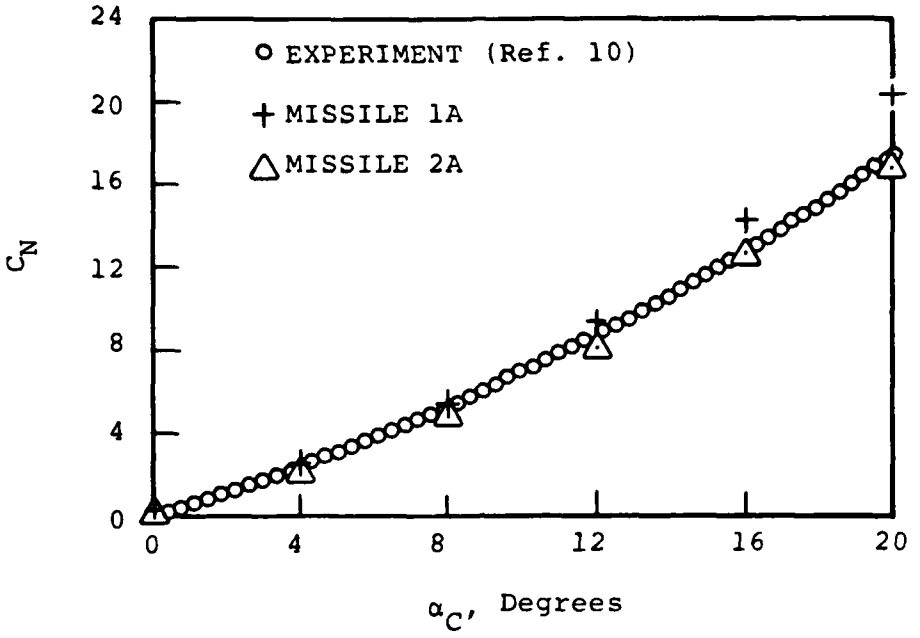

(a) Normal-force coefficient

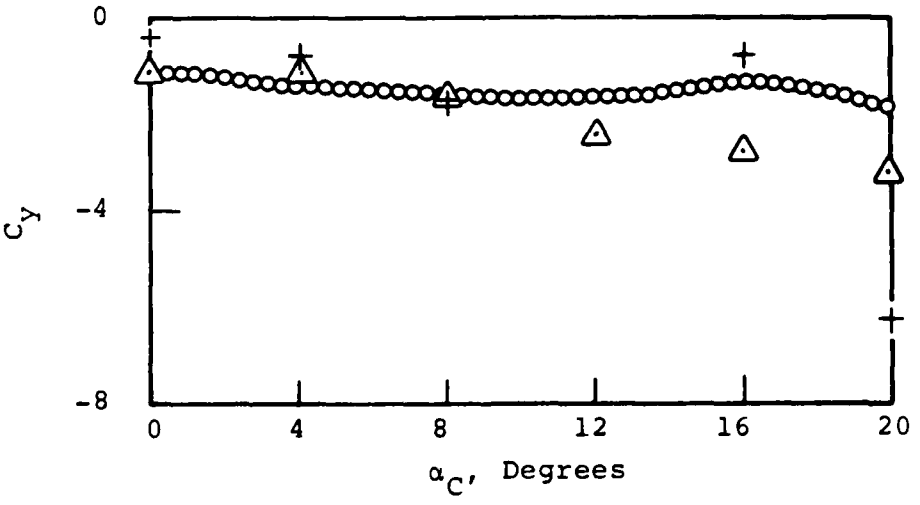

(b) Side-force coefficient

Figure 6. - Comparison of results from new codes with AIM-9L data from reference 10; $M_\infty = 3.5$, $\phi = 0$, $\delta_{1,3} = 20°$, $\delta_{2,4} = 0$.

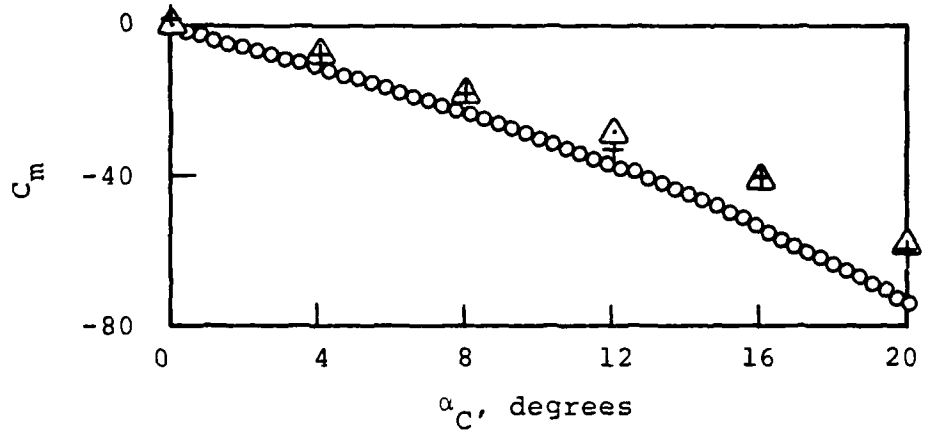

(c) Pitching-moment coefficient

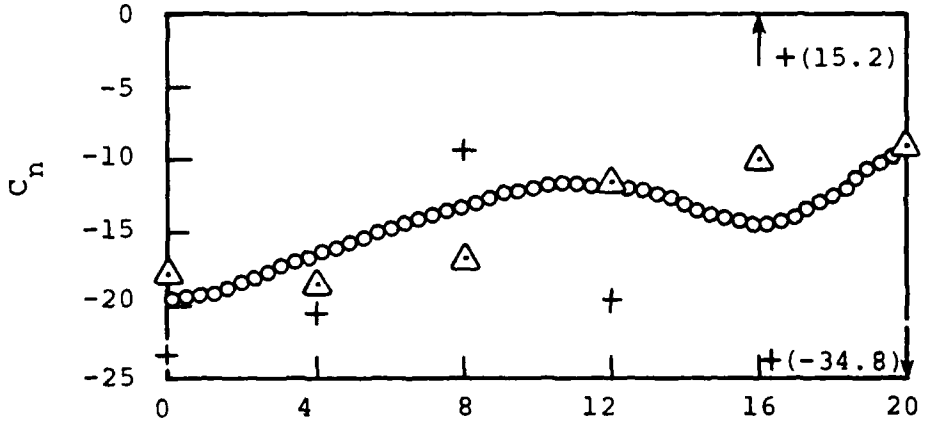

(d) Yawing-moment coefficient

Figure 6. - Continued.

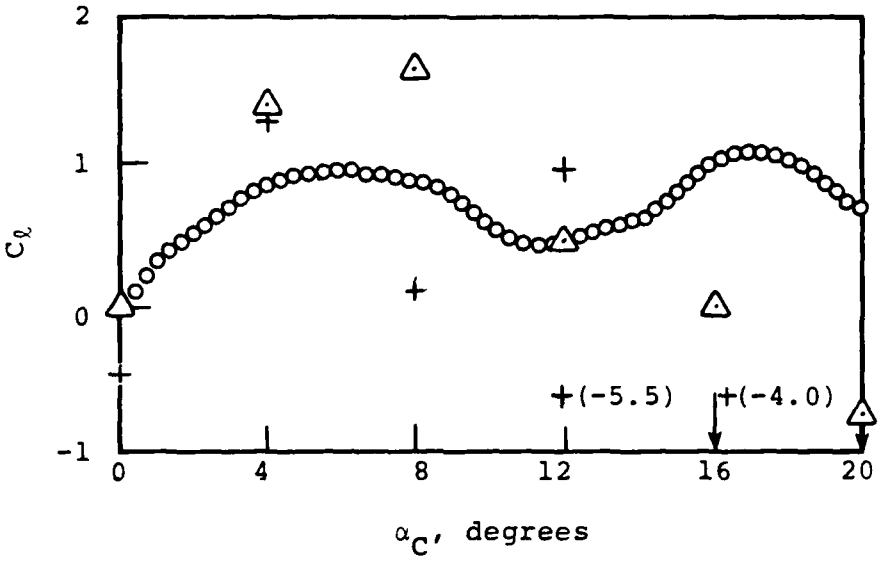

(e) Rolling-moment coefficient

Figure 6. - Concluded.

```
   1
AIM-9L     -     MISL1A TEST CASE
    4     1   11     1    2     1   15     2    2     1    T     F    F
3.50        0.75        .4418       7.983       .375        0.3         14.          1.5
3.35
0.0         1.5
0.0         .375
20.0
0.0
20.0        0.0         20.0        0.0         0.0         0.0         0.0          0.0
1.656       2.225       2.768       2.768
.05         .0005       0.2         1.2         45.0        12.875      1.5
1.744       12.875      14.244      16.700      0.0
  999
```

(a) MISSILE1A

Figure 7.- Sample input cards for the new codes.

```
    1
 AIM-9L     -    MISL2A TEST CASE
     4     1   11     1    2     1    2     2    1     1    0     2   20     T    F    F
3.50         0.75        .4418       7.983       .375        0.3         14.         1.5
3.35
0.0          1.5
0.0          .375
20.0
0.0
20.0         0.0         20.0        0.0
1.656        2.225       2.768       2.768
12.875       16.7
1.0      E+5
0.01         0.0
     0     0    0     3
    1
0.5
0.0
    2
0.216        0.771
0.0225       0.0225
0.0          0.0
1.744        12.875      14.244      16.700      0.0
0.0          0.0         0.0         0.0
  999
```

(b) MISSILE2A

Figure 7.- Concluded.

CALCULATION OF AERODYNAMIC LOADS ON A CRUCIFORM MISSILE

AIM-9L - MISL1A TEST CASE

********** MISSILE BODY GEOMETRY **********

MISSILE IS A CANARD-TAIL COMBINATION

*** NOSE GEOMETRY ***

NOSE TIP RADIUS	NOSE HALF ANGLE
.30000	14.00000

NOSE COORDINATES

XNOSE 0.000 1.500

RNOSE 0.000 .375

LINEAR NORMAL FORCE COEFFICIENT SLOPE IS 3.350

*** CANARD GEOMETRY ***

ASPECT RATIO	SEMISPAN	HINGE LINE	ROOT LEADING EDGE	TIP LEADING EDGE	TRAILING EDGE
4.04101	1.65600	2.22500	1.50000	2.76800	2.76800

*** BODY GEOMETRY ***

BODY RADIUS .37500 CENTER OF MOMENTS 7.98300

*** TAIL GEOMETRY ***

ALPECT RATIO	SEMISPAN	HINGE LINE	ROOT LEADING EDGE	TIP LEADING EDGE	TRAILING EDGE	PHIT
.87184	1.74400	12.87500	12.87500	14.24400	16.70000	0.000

(a) MISSILE1A

Figure 8.- Sample output results for the new codes.

```
**********  REFERENCE LENGTHS AND AREAS  **********

     REFERENCE LENGTHS

OUTPUT LENGTH =      .75000

CPXRC =    1.24800     CPYRC =    1.28100

CPXRT =    3.82500     CPYRT =    1.36900

     REFERENCE AREAS

OUTPUT AREA =      .44180

CANARD WING-ALONE REF. AREA =    1.62431

TAIL WING-ALONE REF. AREA =    8.59869

FIN CN IS NORMALIZED BY OUTPUT AREA.

FIN CPX IS NORMALIZED BY OUTPUT LENGTH.

FIN CPY IS NORMALIZED BY OUTPUT LENGTH AND IS MEASURED FROM BODY AXIS.

**********  FLIGHT CONDITIONS  **********

     MACH NUMBER      TURBULENT FLOW      CANARD DEFLECTION ANGLES      TAIL DEFLECTION ANGLES
       3.500                T              PANEL      ANGLE              PANEL      ANGLE
                                             1         20.0                1         0.0
                                             2          0.0                2         0.0
                                             3         20.0                3         0.0
                                             4          0.0                4         0.0

ANGLES OF ATTACK      20.00

     ROLL ANGLES      0.00

**********  PROGRAM OPERATION  **********

      RVOA    NXOUTB      NI       DXI       EPS       OMEGA      RVORT     RCOMB
     1.200       15       11      .050     .00050      45.000       .20      1.50

NOSE VORTICES ARE RUN TO CANARD TRAILING EDGE
```

(a) MISSILE1A

Figure 8.- Continued.

THE FOLLOWING LOAD CALCULATIONS ARE FOR ALPHA = 20.000 AND PHI = 0.000

********** CONTRIBUTION OF NOSE SECTION TO TOTAL LOADS **********

NOSE VORTICES HAVE FORMED AT X/A = 2.62500

STRENGTHS AND POSITIONS OF VORTICES AT LEADING EDGE OF CANARD ROOT CHORD

I	GAMMA/2PIVA	YO/A	ZO/A
1	.02091	.5555	1.2353
2	-.02091	-.5555	1.2353

NORMAL FORCE COEFFICIENT AND PITCHING MOMENT COEFFICIENT
IN UNROLLED BODY COORDINATES

CZO	CMYO
1.28140	11.88368

CL = 1.284

CD = .478

(a) MISSILE1A

Figure 8.- Continued.

********** CANARD SECTION RESULTS FOR ALPHA = 20.000 AND PHI = 0.000 **********

VORTEX-FREE FIN LOADS

PANEL	ALPHAEQ	CN	CPY
1	18.90	.8259	1.0835
2	20.33	.8973	1.0854
3	18.90	.8259	1.0835
4	20.33	.8973	1.0854

	FIN 1	FIN 2	FIN 3	FIN 4
VORTEX INDUCED EQUIVALENT ANGLE OF ATTACK, DEGREES	0.00	-.04	0.00	-.04
CENTER OF PRESSURE FOR VORTEX INDUCED LOADS	0.00	1.99	0.00	1.99

FIN LOADING INFORMATION

PANEL	ETA	AEBYAL	AL/A
1	.3416	.0638	1.3807
2	.3428	.0742	1.4755
3	.3416	.0638	1.3807
4	.3428	.0742	1.4755

TRAILING VORTEX INFORMATION

K	GAMC	YSPAN	YO	ZO
1	.1169	2.7665	.4952	2.7665
2	-.1261	2.7753	-2.7753	0.0000
3	-.1169	2.7665	.4952	-2.7665
4	.1261	2.7753	2.7753	0.0000

*** TOTAL CANARD FIN LOADS INCLUDING VORTEX EFFECTS ***

PANEL	ALPHAEQ	CN	CPX	CPY	CRM	CAM	CHM
1	18.90	.8259	.9883	1.0835	.8409	.4819	-.0179
2	20.29	.8957	.9899	1.0856	.9723	.5245	-.0208
3	18.90	.8259	.9883	1.0835	.8409	.4819	-.0179
4	20.29	.8957	.9899	1.0856	.9723	.5245	-.0208

*** CONTRIBUTION OF CANARD SECTION TO TOTAL LOADS ***

UNROLLED COORDINATES

CXO = .5650 CMXO = 0.0000

CYO = -1.8846 CMYO = 17.8066

CZO = 2.3917 CMZO = 13.9651

CL = 2.0542

CD = 1.3489

ROLLED COORDINATES

CX = .5650 CMX = 0.0000

CY = -1.8846 CMY = 17.8066

CZ = 2.3917 CMZ = 13.9651

(a) MISSILE1A

Figure 8.- Continued.

********** AFTERBODY SECTION RESULTS FOR ALPHA = 20.000 AND PHI = 0.000 **********
***** VORTEX TRACKING RESULTS OVER AFTERBODY *****

X/A	I	GAMMA(I)	YO(I)/A	ZO(I)/A	FLOANG	THETA	NORMAL FORCE	SIDE FORCE
.7381E+01	1	.1169E+00	.4952E+00	.2767E+01	15.70	71.94		
	2	-.1261E+00	-.2775E+01	0.				
	3	-.1169E+00	.4952E+00	-.2767E+01				
	4	.1261E+00	.2775E+01	0.				

*** AFTERBODY VORTICES HAVE FORMED AT X/A = 7.38

THE LEFT VORTEX POSITION IS YO/A =***** AND ZO/A = .410

THE RIGHT VORTEX POSITION IS YO/A =1.128 AND ZO/A = .410

.9178E+01	1	.1169E+00	.5187E+00	.3275E+01	16.27	72.43	.1034	.0286
	2	-.1261E+00	-.2713E+01	.6755E+00				
	3	-.1169E+00	.5028E+00	-.2278E+01				
	4	.1261E+00	.2837E+01	.6682E+00				
	5	-.3509E-01	-.7134E+00	.1015E+01				
	6	.1228E-01	.9554E+00	.9140E+00				
.1097E+02	1	.1169E+00	.5446E+00	.3785E+01	17.34	72.83	.1062	.0418
	2	-.1261E+00	-.2622E+01	.1343E+01				
	3	-.1169E+00	.5202E+00	-.1825E+01				
	4	.1261E+00	.2882E+01	.1324E+01				
	5	-.7091E-01	-.2875E+00	.1335E+01				
	6	.3404E-01	.8644E+00	.1256E+01				
.1277E+02	1	.1169E+00	.5748E+00	.4293E+01	18.82	73.15	.0960	.0409
	2	-.1261E+00	-.2513E+01	.1990E+01				
	3	-.1169E+00	.5781E+00	-.1424E+01				
	4	.1261E+00	.2919E+01	.1969E+01				
	5	-.1150E+00	.9670E-02	.1521E+01				
	6	.6574E-01	.8587E+00	.1472E+01				
.1457E+02	1	.1169E+00	.6072E+00	.4799E+01	20.74	74.87	.1267	.0076
	2	-.1261E+00	-.2395E+01	.2618E+01				
	3	-.1169E+00	.7466E+00	-.1050E+01				
	4	.1261E+00	.2952E+01	.2605E+01				
	5	-.1679E+00	.5145E-01	.1625E+01				
	6	.1077E+00	.8524E+00	.1567E+01				

VORTEX 3 HAS BEEN COMBINED WITH THE RIGHT AFTERBODY VORTEX.

.1457E+02	1	.1169E+00	.6072E+00	.4799E+01	17.24	86.27	.1267	.0076
	2	-.1261E+00	-.2395E+01	.2618E+01				
	3	.1261E+00	.2952E+01	.2605E+01				
	4	-.1679E+00	.5145E-01	.1625E+01				

(a) MISSILE1A

Figure 8.- Continued.

	5	-.9171E-02	.8524E+00	.1567E+01				
.1437E+02	1	.1169E+00	.6592E+00	.5307E+01	17.81	86.80	.1479	.0709
	2	-.1261E+00	-.2288E+01	.3253E+01				
	3	.1261E+00	.2986E+01	.3196E+01				
	4	-.2030E+00	-.4806E-01	.1922E+01				
	5	.2862E-01	.6161E+00	.1634E+01				
.1816E+02	1	.1169E+00	.7100E+00	.5808E+01	18.25	87.15	.1173	.0898
	2	-.1261E+00	-.2173E+01	.3883E+01				
	3	.1261E+00	.3024E+01	.3787E+01				
	4	-.2453E+00	-.1402E+00	.2221E+01				
	5	.8722E-01	.2787E+00	.1748E+01				
.1996E+02	1	.1169E+00	.7598E+00	.6304E+01	18.59	87.39	.1090	.0719
	2	-.1261E+00	-.2048E+01	.4504E+01				
	3	.1261E+00	.3066E+01	.4379E+01				
	4	-.3246E+00	-.2867E+00	.2550E+01				
	5	.2058E+00	-.6103E-01	.1958E+01				
.2176E+02	1	.1169E+00	.8080E+00	.6789E+01	18.85	87.58	.1564	-.0712
	2	-.1261E+00	-.1906E+01	.5118E+01				
	3	.1261E+00	.3109E+01	.4976E+01				
	4	-.5730E+00	-.5970E+00	.2903E+01				
	5	.5631E+00	-.4214E+00	.2261E+01				
.2355E+02	1	.1169E+00	.8453E+00	.7256E+01	19.06	87.75	.4278	-.4845
	2	-.1261E+00	-.1718E+01	.5696E+01				
	3	.1261E+00	.3142E+01	.5589E+01				
	4	-.9806E+00	-.1267E+01	.3133E+01				
	5	.1118E+01	-.9395E+00	.2515E+01				
.2535E+02	1	.1169E+00	.8594E+00	.7715E+01	19.22	87.94	.6275	-.7896
	2	-.1261E+00	-.1538E+01	.6159E+01				
	3	.1261E+00	.3171E+01	.6228E+01				
	4	-.1139E+01	-.2011E+01	.3095E+01				
	5	.1323E+01	-.1470E+01	.2567E+01				
.2715E+02	1	.1169E+00	.8627E+00	.8180E+01	19.33	88.10	.6812	-.8982
	2	-.1261E+00	-.1439E+01	.6584E+01				
	3	.1261E+00	.3202E+01	.6883E+01				
	4	-.1215E+01	-.2556E+01	.2848E+01				
	5	.1416E+01	-.1831E+01	.2453E+01				
.2894E+02	1	.1169E+00	.8660E+00	.8651E+01	19.43	88.23	.7470	-.9278
	2	-.1261E+00	-.1381E+01	.7031E+01				
	3	.1261E+00	.3234E+01	.7550E+01				
	4	-.1260E+01	-.2840E+01	.2487E+01				
	5	.1470E+01	-.1964E+01	.2255E+01				
.3074E+02	1	.1169E+00	.8737E+00	.9121E+01	19.50	88.34	.8928	-.8920

(a) MISSILE1A

Figure 8.- Continued.

	2	-.1261E+00	-.1331E+01	.7497E+01				
	3	.1261E+00	.3263E+01	.8222E+01				
	4	-.1291E+01	-.2870E+01	.2087E+01				
	5	.1504E+01	-.1856E+01	.2030E+01				
.3254E+02	1	.1169E+00	.8874E+00	.9586E+01	19.56	88.43	1.2334	-.7384
	2	-.1261E+00	-.1278E+01	.7969E+01				
	3	.1261E+00	.3287E+01	.8897E+01				
	4	-.1313E+01	-.2677E+01	.1682E+01				
	5	.1527E+01	-.1493E+01	.1810E+01				
.3433E+02	1	.1169E+00	.9090E+00	.1004E+02	19.62	88.51	2.3116	-.2247
	2	-.1261E+00	-.1216E+01	.8438E+01				
	3	.1261E+00	.3303E+01	.9571E+01				
	4	-.1331E+01	-.2317E+01	.1236E+01				
	5	.1544E+01	-.7292E+00	.1593E+01				

*** CONTRIBUTION OF AFTERBODY SECTION TO TOTAL LOADS IN UNROLLED BODY COORDINATES **

CYO = -4.675 CMYO = -26.342

CZO = 9.612 CMZO = 17.036

CL = 9.033

CD = 3.288

(a) MISSILE1A

Figure 8.- Continued.

********** TAIL SECTION RESULTS FOR ALPHA = 20.000 AND PHI = 0.000 **********

VORTEX-FREE FIN LOADS

PANEL	ALPHAEQ	CN	CPY
1	-.00	-.0000	1.3039
2	20.09	4.3539	1.3107
3	-.00	-.0000	1.3039
4	20.09	4.3539	1.3107

	FIN 1	FIN 2	FIN 3	FIN 4
VORTEX INDUCED EQUIVALENT ANGLE OF ATTACK, DEGREES	.58	-13.01	-2.86	-.81
CENTER OF PRESSURE FOR VORTEX INDUCED LOADS	11.34	2.10	2.34	2.18

*** TOTAL TAIL FIN LOADS INCLUDING VORTEX EFFECTS ***

PANEL	ALPHAEQ	CN	CPX	CPY	CRM	CRM	CHM
1	.58	.0959	2.3133	5.6709	.5439	.4960	-.2219
2	7.67	1.3816	2.3977	1.8702	2.5838	1.8930	-3.3126
3	-2.86	-.4736	2.3381	1.1678	-.5531	-.3163	1.1074
4	19.37	4.1668	2.5391	1.3207	5.5030	3.4196	*******

*** CONTRIBUTION OF TAIL SECTION TO TOTAL LOADS ***

UNROLLED COORDINATES				ROLLED COORDINATES			
CX0 =	0.0000	CMX0 =	4.0162	CX =	0.0000	CMX =	4.0162
CY0 =	.4241	CMY0 =	-62.7186	CY =	.4241	CMY =	-62.7186
CZ0 =	6.8837	CMZ0 =	3.8054	CZ =	6.8837	CMZ =	3.8054
CL =	6.4685						
CD =	2.3544						

*** SUMMARY OF TOTAL LOADS IN BODY COORDINATES ***

ALPHA = 20.000 PHI = 0.000

UNROLLED COORDINATES				ROLLED COORDINATES			
CX0 =	.56497	CMX0 =	4.01617	CX =	.56497	CMX =	4.01617
CY0 =	-6.13557	CMY0 =	-59.37076	CY =	-6.13557	CMY =	-59.37076
CZ0 =	20.16906	CMZ0 =	34.80650	CZ =	20.16906	CMZ =	34.80650
CL =	18.75949	CPX =	13.58766				
CD =	7.42912	CPY =	4.97110				

(a) MISSILE1A

Figure 8.- Continued.

CALCULATION OF AERODYNAMIC LOADS ON A CRUCIFORM MISSILE

AIM-9L - MISL2A TEST CASE

********** MISSILE BODY GEOMETRY **********

MISSILE IS A CANARD-TAIL COMBINATION

*** NOSE GEOMETRY ***

NOSE TIP RADIUS	NOSE HALF ANGLE	NOSE COORDINATES	
		XNOSE	RNOSE
.30000	14.00000	0.000	0.000
		1.500	.375

LINEAR NORMAL FORCE COEFFICIENT SLOPE IS 3.350

*** CANARD GEOMETRY ***

ASPECT RATIO	SEMISPAN	HINGE LINE	ROOT LEADING EDGE	TIP LEADING EDGE	TRAILING EDGE
4.04101	1.65600	2.22500	1.50000	2.76800	2.76800

(b) MISSILE2A

Figure 8.- Continued.

*** BODY GEOMETRY ***

BODY RADIUS	BODY LENGTH
.375	16.700

SOURCE DISTRIBUTION

XSRC	QS
8.350	0.000

BODY SHAPE

X	R	DR
3.607	.376	0.000
12.876	.376	0.000

*** TAIL GEOMETRY ***

ASPECT RATIO	SEMISPAN	HINGE LINE	ROOT LEADING EDGE	TIP LEADING EDGE	TRAILING EDGE	PHIT
.87184	1.74400	12.87500	12.87500	14.24400	16.70000	0.000

********** REFERENCE LENGTHS AND AREAS **********

REFERENCE LENGTHS

OUTPUT LENGTH = .75000

CPXRC = 1.24800 CPYRC = 1.28100

CPXRT = 3.82500 CPYRT = 1.36900

MOMENT CENTER IS AT X = 7.983

REFERENCE AREAS

OUTPUT AREA = .44180

CANARD WING-ALONE REF. AREA = 1.62431

TAIL WING-ALONE REF. AREA = 8.59869

FIN CN IS NORMALIZED BY OUTPUT AREA.

FIN CPX IS NORMALIZED BY OUTPUT LENGTH.

FIN CPY IS NORMALIZED BY OUTPUT LENGTH AND IS MEASURED FROM BODY AXIS.

(b) MISSILE2A

Figure 8.- Continued.

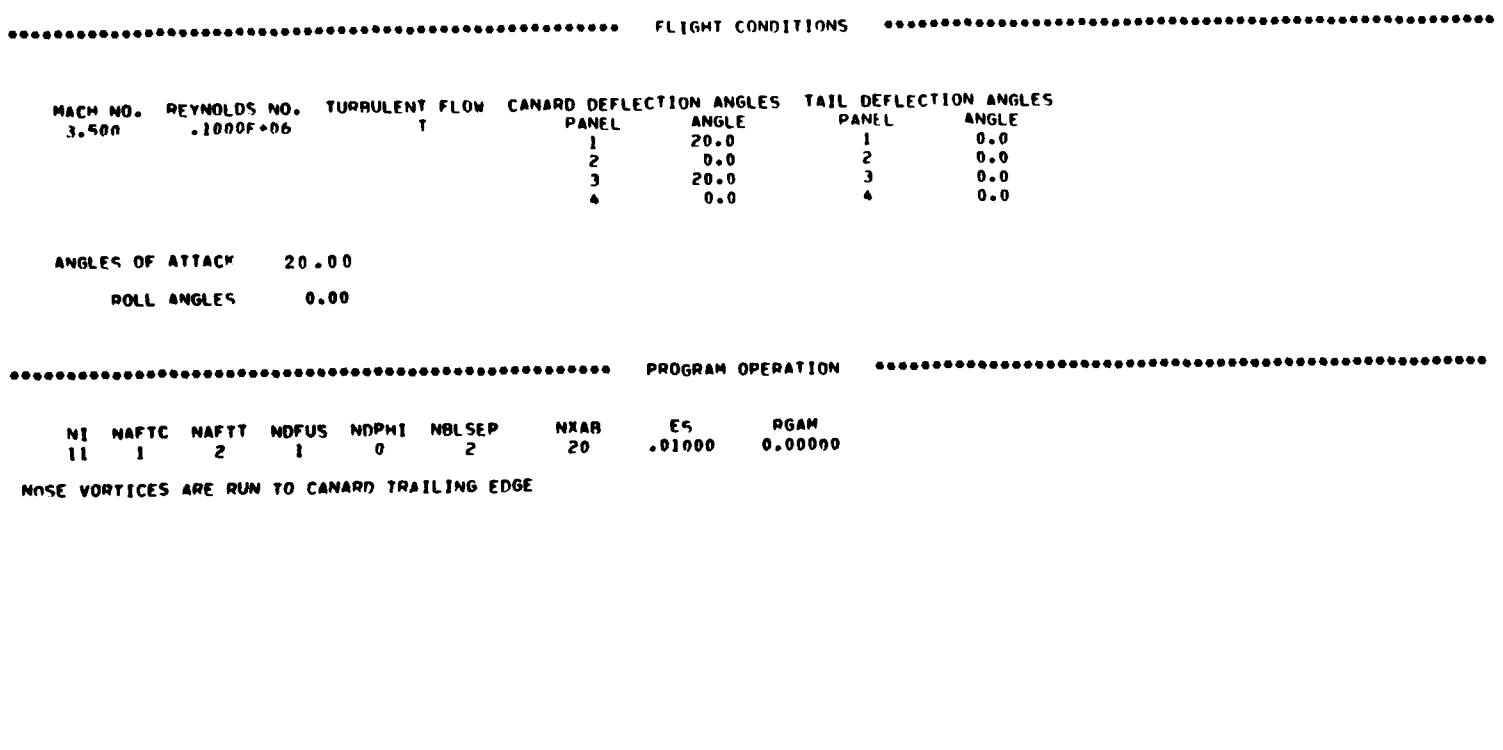

FLIGHT CONDITIONS

MACH NO.	REYNOLDS NO.	TURBULENT FLOW
3.500	.1000E+06	T

CANARD DEFLECTION ANGLES		TAIL DEFLECTION ANGLES	
PANEL	ANGLE	PANEL	ANGLE
1	20.0	1	0.0
2	0.0	2	0.0
3	20.0	3	0.0
4	0.0	4	0.0

ANGLES OF ATTACK 20.00

ROLL ANGLES 0.00

PROGRAM OPERATION

NI	NAFTC	NAFTT	NDFUS	NDPHI	NBLSEP	NXAB	ES	RGAM
11	1	2	1	0	2	20	.01000	0.00000

NOSE VORTICES ARE RUN TO CANARD TRAILING EDGE

(b) MISSILE2A

Figure 8.- Continued.

WING-ALONE CURVE FOR FIRST SET OF FINS (REF. AREA IS PLANFORM AREA OF ONE FIN)

ALPHA	CNW
0.0	0.000
2.0	.041
4.0	.081
6.0	.125
8.0	.173
10.0	.221
12.0	.267
14.0	.316
16.0	.367
18.0	.424
20.0	.480
22.0	.530
24.0	.580
26.0	.635
28.0	.694
30.0	.754
32.0	.795
34.0	.835
36.0	.883
38.0	.937
40.0	.991
42.0	1.045
44.0	1.100
46.0	1.150
48.0	1.195
50.0	1.240
52.0	1.284
54.0	1.329
56.0	1.371
58.0	1.411
60.0	1.451

(b) MISSILE2A

Figure 8.- Continued.

WING-ALONE CURVE FOR SECOND SET OF FINS (REF. AREA IS PLANFORM AREA OF ONE FIN)

ALPHA	CNW
0.0	0.000
2.0	.034
4.0	.069
6.0	.107
8.0	.149
10.0	.192
12.0	.239
14.0	.288
16.0	.339
18.0	.392
20.0	.445
22.0	.501
24.0	.559
26.0	.617
28.0	.674
30.0	.732
32.0	.792
34.0	.854
36.0	.916
38.0	.981
40.0	1.044
42.0	1.109
44.0	1.172
46.0	1.230
48.0	1.282
50.0	1.332
52.0	1.373
54.0	1.413
56.0	1.448
58.0	1.480
60.0	1.510

(b) MISSILE2A

Figure 8.- Continued.

```
 THE FOLLOWING LOAD CALCULATIONS ARE FOR ALPHA = 20.000   AND PHI =   0.000
**************************************  CONTRIBUTION OF NOSE SECTION TO TOTAL LOADS  **************************************

 NOSE VORTICES HAVE FORMED AT X/A =    2.62500

          STRENGTHS AND POSITIONS OF VORTICES AT LEADING EDGE OF CANARD ROOT CHORD

                I    GAMMA/2PIVA     Y0/A      Z0/A
                1      .02091        .5555     1.2353
                2     -.02091       -.5555     1.2353


          NORMAL FORCE COEFFICIENT AND PITCHING MOMENT COEFFICIENT
               IN UNWOLLED BODY COORDINATES

            CZO              CMYO

          1.24931          11.95454

            CL =  1.212

            CD =   .441
```

(b) MISSILE2A

Figure 8.- Continued.

•••••••••••••••••••••••••••••••••• CANARD SECTION RESULTS FOR ALPHA = 20.000 AND PHI = 0.000 ••••••••••••••••••••••••••••••••••

VORTEX-FREE FIN LOADS

PANEL	ALPHAEQ	CN	CPY
1	18.90	.8259	1.0835
2	20.33	.8973	1.0854
3	18.90	.8259	1.0835
4	20.33	.8973	1.0854

	FIN 1	FIN 2	FIN 3	FIN 4
VORTEX INDUCED EQUIVALENT ANGLE OF ATTACK, DEGREES	0.00	-.04	0.00	-.04
CENTER OF PRESSURE FOR VORTEX INDUCED LOADS	0.00	1.99	0.00	1.99

FIN LOADING INFORMATION

PANEL	ETA	AEBYAL	AL/A
1	.3416	.0638	1.3807
2	.3428	.0742	1.4755
3	.3416	.0638	1.3807
4	.3428	.0742	1.4755

TRAILING VORTEX INFORMATION

K	GAMC	YSPAN	YO	ZO
1	.1169	2.7665	.4952	2.7665
2	-.1261	2.7753	-2.7753	0.0000
3	-.1169	2.7665	.4952	-2.7665
4	.1261	2.7753	2.7753	0.0000

••• TOTAL CANARD FIN LOADS INCLUDING VORTEX EFFECTS •••

PANEL	ALPHAEQ	CN	CPX	CPY	CRM	CHM	CMM
1	18.90	.8259	.9883	1.0835	.8409	.4819	-.0179
2	20.29	.8957	.9899	1.0856	.9723	.5245	-.0208
3	18.90	.8259	.9883	1.0835	.8409	.4819	-.0179
4	20.29	.8957	.9899	1.0856	.9723	.5245	-.0208

••• CONTRIBUTION OF CANARD SECTION TO TOTAL LOADS •••

UNROLLED COORDINATES				ROLLED COORDINATES			
CXO =	.5650	CMXO =	0.0000	CX =	.5650	CMX =	0.0000
CYO =	-1.8846	CMYO =	17.9051	CY =	-1.8846	CMY =	17.9051
CZO =	2.4043	CMZO =	13.9651	CZ =	2.4043	CMZ =	13.9651

(b) MISSILE2A

Figure 8.- Continued.

```
                                    CL =   2.0661
                                    CD =   1.3532

 FOR AFTERBODY VORTEX CALCULATIONS THE FOLLOWING VARIABLES ARE USED
      VORTEX REDUCTION FACTOR (VRF) =  .437
      INITIAL RADIUS (FMKF)         = 1.100
      SEPARATION FACTOR (FACTS)     =  .0110
```

(b) MISSILE2A

Figure 8.- Continued.

X	CN(X)	CY(X)	(+Y SEPARATION POINT) Y	Z	BETA	(-Y SEPARATION POINT) Y	Z	BETA	(+Y VORTICITY CENTROID) GAM/V	Y	Z	(-Y VORTICITY CENTROID) GAM/V	Y	Z
0.000	0.00	0.00	2.77	-.00	.0	.37	.09	101.5	-.365	.09	256.37	0.000	0.00	0.00
-.052	-.30	.31	3.27	-.06	-.0	.37	.07	100.7	-.369	.07	259.18	.052	.31	.30
-.103	-.26	.36	3.78	-.08	-.0	.37	.06	99.0	-.371	.06	260.67	.101	.27	.36
-.155	-.24	.40	4.28	-.09	-.0	.37	.05	97.3	-.372	.05	262.36	.148	.25	.40
-.207	-.22	.44	4.79	-.10	-.0	.37	.04	96.3	-.373	.04	263.49	.194	.24	.44
-.258	-.21	.48	5.29	-.10	-.1	.37	.04	95.6	-.374	.04	264.26	.237	.23	.48
-.310	-.19	.51	5.80	-.11	-.1	.37	.03	95.2	-.374	.03	264.83	.280	.22	.52
-.362	-.18	.54	6.31	-.11	-.1	.37	.03	94.7	-.374	.03	265.57	.320	.22	.55
-.413	-.18	.57	6.81	-.11	-.1	.37	.03	94.3	-.375	.02	266.28	.360	.21	.58
-.464	-.17	.60	7.32	-.11	-.1	.37	.03	94.0	-.375	.02	266.94	.399	.21	.60
-.515	-.17	.62	7.82	-.11	-.1	.37	.03	93.8	-.375	.02	267.68	.437	.20	.62
-.564	-.17	.64	8.33	-.11	-.1	.37	.02	93.7	-.375	.01	268.26	.475	.20	.63
-.613	-.17	.67	8.83	-.10	-.1	.37	.02	93.7	-.375	.01	268.75	.513	.19	.64
-.662	-.17	.69	9.34	-.10	-.1	.37	.02	93.6	-.376	.01	269.17	.551	.18	.65
-.710	-.18	.72	9.84	-.08	-.1	.37	.02	93.4	-.376	.00	269.54	.588	.17	.66
-.757	-.19	.74	10.35	-.09	-.0	.37	.02	93.2	-.376	.00	269.94	.625	.16	.67
-.804	-.20	.77	10.85	-.09	-.0	.37	.02	93.2	-.375	-.01	271.07	.662	.14	.68
-.848	-.21	.80	11.36	-.06	-.0	.37	.02	93.4	-.375	-.01	272.08	.700	.13	.69
-.891	-.22	.84	11.86	-.09	.0	.37	.02	93.4	-.375	-.02	272.82	.738	.13	.70
-.932	-.22	.88	12.37	-.08	.0	.37	.02	92.9	-.375	-.02	273.13	.777	.12	.71
-.972	-.22	.93	12.88	-.10	.0	.38	.01	92.2	-.375	-.02	272.66	.816	.12	.72

********** AFTERBODY SECTION RESULTS FOR ALPHA = 20.000 AND PHI = 0.000 **********

*** CONTRIBUTION OF AFTERBODY SECTION TO TOTAL LOADS IN UNROLLED BODY COORDINATES **

CYO = -.660 CMYO = .732

CZO = 3.398 CMZO = .723

(b) MISSILE2A

Figure 8.- Continued.

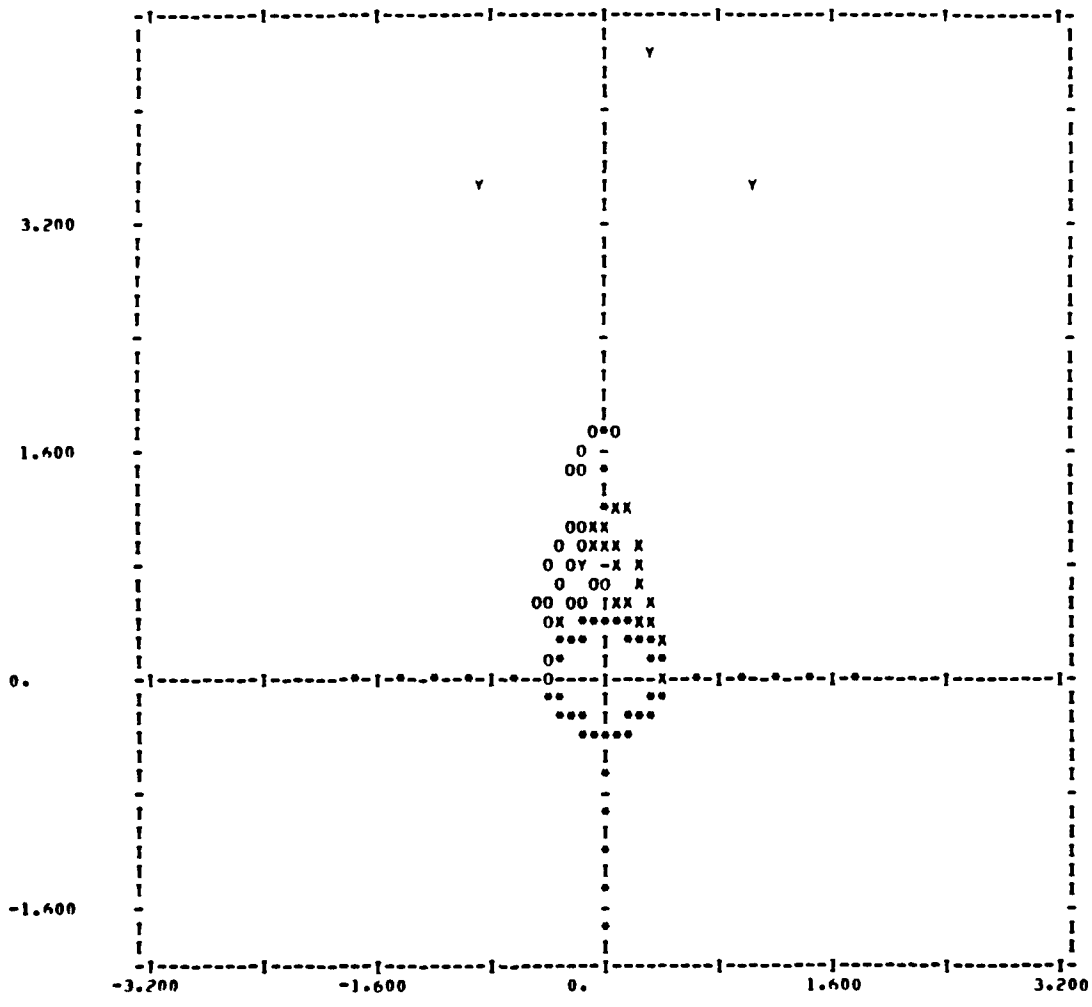

(b) MISSILE2A

Figure 8.- Continued.

•••••••••••••••••••••••••••••••••• TAIL SECTION RESULTS FOR ALPHA = 20.000 AND PHI = 0.000 ••••••••••••••••••••••••••••••••••

VORTEX-FREE FIN LOADS

PANEL	ALPHAEQ	CN	CPY
1	-.00	-.0000	1.3039
2	20.09	4.3539	1.3107
3	-.00	-.0000	1.3039
4	20.09	4.3539	1.3107

	FIN 1	FIN 2	FIN 3	FIN 4
VORTEX INDUCED EQUIVALENT ANGLE OF ATTACK, DEGREES	3.31	-1.79	.06	-1.21
CENTER OF PRESSURE FOR VORTEX INDUCED LOADS	2.36	2.14	3.12	2.30

••• TOTAL TAIL FIN LOADS INCLUDING VORTEX EFFECTS •••

PANEL	ALPHAEQ	CN	CPX	CPY	CRM	CRM	CHM
1	3.31	.5497	2.3431	1.1815	.6495	.3746	-1.2880
2	18.50	3.9413	2.5309	1.3362	5.2663	3.2956	-9.9750
3	.06	.0092	2.3076	1.5601	.0143	.0097	-.0211
4	19.02	4.0748	2.5357	1.3216	5.3854	3.3479	*******

••• CONTRIBUTION OF TAIL SECTION TO TOTAL LOADS •••

UNROLLED COORDINATES				ROLLED COORDINATES			
CX0 =	0.0000	CMX0 =	.7543	CX =	0.0000	CMX =	.7543
CY0 =	-.6275	CMY0 =	-88.5576	CY =	-.6275	CMY =	-88.5576
CZ0 =	9.6926	CMZ0 =	-5.6292	CZ =	9.6926	CMZ =	-5.6292
CL =	9.1081						
CD =	3.3151						

(b) MISSILE2A

Figure 8.- Continued.

*** SUMMARY OF TOTAL LOADS ***
ALPHA = 20.00 PHI = 0.00

	UNROLLED COORDINATES						*** BODY AXIS COORDINATES					
	CXO	CYO	CZO	CMXO	CMYO	CMZO	CX	CY	CZ	CMX	CMY	CMZ
NOSE	0.00000	0.00000	1.28931	0.00000	11.95454	0.00000	0.00000	0.00000	1.28931	0.00000	11.95454	0.00000
CANARD	.56497	-1.88461	2.40433	0.00000	17.90514	13.96512	.56497	-1.88461	2.40433	0.00000	17.90514	13.96512
AFTERBODY	0.00000	-.65977	3.39841	0.00000	.73179	.72346	0.00000	-.65977	3.39841	0.00000	.73179	.72346
TAIL	0.00000	-.62745	9.69262	.75426	-88.55759	-5.62923	0.00000	-.62745	9.69262	.75426	-88.55759	-5.62923
TOTALS	.56497	-3.17184	16.78466	.75426	-57.96612	9.05935	.56497	-3.17184	16.78466	.75426	-57.96612	9.05935

AXIAL CENTERS OF PRESSURE

NORMAL FORCE (CPX) = 14.09752

SIDE FORCE (CPY) = 7.78782

END OF CALCULATIONS FOR ALPHA SWEEP AT PHI = 0.000

END OF CALCULATIONS FOR THIS CASE

***** END OF RUN *****

(b) MISSILE2A

Figure 8.- Concluded.


FILMED
82